Post-trauma behavioral phenotype predicts the degree of vulnerability to fear relapse after extinction in male rats

Fanny Demars, Ralitsa Todorova, Gabriel Makdah, Antonin Forestier, Marie-Odile Krebs, Bill P Godsil, Thérèse M Jay, Sidney I Wiener, Marco N Pompili

Post-trauma behavioral phenotype predicts the degree of vulnerability to fear relapse after extinction in male rats

Fanny Demars[1,*], Ralitsa Todorova[2], Gabriel Makdah[2,3], Antonin Forestier[1,4], Marie-Odile Krebs[1], Bill P. Godsil[1], Thérèse M. Jay[1], Sidney I. Wiener[2], & Marco N. Pompili[1,2,5,6,*,§]

[1] Institut de Psychiatrie et Neurosciences de Paris (IPNP) - INSERM U1266, Institut de Psychiatrie - CNRS GDR3557, GHU Psychiatrie Neurosciences, Université de Paris, 102-108 Rue de la Santé, 75014 Paris, France
[2] Centre Interdisciplinaire de Recherche en Biologie (CIRB) - CNRS UMR 7241 - INSERM U1050, Collège de France, Université PSL, 11 place Marcelin Berthelot, 75005 Paris, France
[3] Hospices Civils de Lyon, Faculté de Médecine Lyon Est, Université Claude Bernard, Lyon, France
[4] Ecole Nationale Vétérinaire d'Alfort, Maisons-Alfort, France
[5] Current address: Institut de Neurosciences des Systèmes (INS) – INSERM UMR1106, Aix-Marseille Université, 27 Boulevard Jean Moulin, 13005 Marseille, France
[6] Twitter : @MNPompili
[*] Equal first authors
[§] Lead contact, correspondence: marco.pompili@college-de-france.fr

SUMMARY

Current treatments for trauma-related disorders remain ineffective for many patients[1,2]. Fear extinction deficiency is a prominent feature of these diseases[3], and many behavioral treatments rely on extinction training[4,5]. However, in many patients, therapy is followed by a relapse of symptoms, and the underpinnings of such interindividual variations in vulnerability to relapse remain unknown[6–8]. Here, we modeled interindividual differences in post-therapy fear relapse with an ethologically-relevant trauma recovery paradigm. After fear conditioning, male rats underwent fear extinction while foraging in a large enriched arena, permitting the expression of a wide spectrum of behaviors. An automated multidimensional behavioral assessment revealed that post-conditioning fear response profiles clustered into two groups: some animals expressed fear by freezing more, while others darted more, as if fleeing from danger. Remarkably, the tendency of an animal to dart or to freeze after CS presentation during the first extinction session was respectively associated with stronger or weaker fear renewal. Moreover, genome-wide transcriptional profiling revealed that these groups differentially regulated specific sets of genes, some of which were previously implicated in anxiety and trauma-related disorders. Our results suggest that post-trauma behavioral phenotypes and the associated gene expression landscapes can serve as markers of fear relapse susceptibility, and thus may be instrumental for future development of more effective treatments for psychiatric patients.

RESULTS

While traditionally freezing behavior is employed as the sole measurement of fear in conditioning and extinction protocols in rodents, recent work also investigated active fear responses after fear conditioning in the form of flight-like behavior, revealing differences between individuals in their propensity for passive vs. active fear responses[9–11]. Such interindividual differences may be useful indicators of the vulnerability to fear relapse after extinction. Nevertheless, rodents display a restricted behavioral repertoire in standard conditioning chambers (Skinner boxes), potentially reducing detectible differences between individuals. In contrast, more ecologically relevant settings would allow expression of a broader repertoire of animals' natural behavioral patterns[12], therefore better modelling and contrasting healthy and pathological behavioral profiles. Despite a recent surge in novel naturalistic approaches to study fear behavior[13–16], biological markers of interindividual differences in the vulnerability to fear relapse after extinction have not yet been revealed.

Here, we hypothesized that soon following fear conditioning, diverse behavioral phenotypes may be unveiled in an enriched naturalistic setting permitting the animals to express a wide spectrum of behaviors. We also hypothesized that these early behavioral markers may predict individual vulnerability to fear relapse.

Complex behavioral patterns in an ethologically-relevant fear extinction paradigm

To test this, we designed an ethologically rich model of trauma recovery where fear extinction takes place in a large open field arena enriched with large objects. There, male rats were habituated to forage for food pellets, then underwent a typical fear conditioning protocol in a standard apparatus, followed by fear extinction training in the arena (**Figure 1A**). We used head movements, orientation and position measures, and machine learning, to automatically classify animal behavior (**Figure 1B**) in six classes: freezing, darting, grooming, object exploration, rearing, and all remaining foraging and exploratory behaviors, referred to collectively as foraging/exploration. During darting, animals run at high speeds in long straight trajectories, as previously observed in extended environments[17] (**Figure 1C-D**). This contrasted with the locomotor patterns associated with foraging, where the animals moved about at low to medium speeds in various directions (**Video S1**).

Following auditory fear conditioning, during fear extinction training in the open field, we observed the expected freezing responses to the conditioned stimulus (CS). Freezing to the CS was initially higher than during habituation, but, after three days of cued fear extinction training in the open field, it was indistinguishable from baseline (**Figure S1A-B**). This demonstrated that cued conditioned fear was also recalled in the open field, and that fear successfully reduced with extinction training. Other behaviors were also affected after conditioning, such as grooming, which was reduced (**Figure S1B**). Importantly, behavioral changes were not uniform among animals and, notably, interindividual variability in the incidence of freezing and darting increased then (**Figure S1A**). This suggested that these behaviors could constitute useful targets for a behavioral profiling after fear conditioning.

Interindividual differences in fear responses during extinction training

Overall, during early extinction, CS presentations elicited highly variable behavioral responses among animals (**Figure 1E**). We hypothesized that this variability corresponded to diverging behavioral phenotypes, which, in turn, would correspond to differing degrees of susceptibility to relapse after extinction. Principal component analysis (PCA) of the expression of the six classes of behavior aimed to characterize this variability of fear responses during early extinction training. This permitted to account for all of the behavioral variance in our data in an unbiased manner. The first principal component (PC1) explained most of the variance (**Figure 1F**), and was characterized by opposing contributions of darting and freezing (**Figure 1G**). By clustering the expression of the three significant PCs in the first extinction session (ext1), animals were divided into distinct groups (**Figure 1H**, **Figure S1C-D**), without any a priori assumptions about which specific behavior would better define behavioral phenotypes. This revealed that the two groups differed mainly by the incidence of freezing and darting in early extinction training (**Figures 2A-B**, **S1E**, and **S2A-H**). Notably, these behavioral profiles emerged on the first extinction session after fear conditioning, and reconverged over the course of extinction training (**Figure 2C-F**), further suggesting that behavioral divergence originated from conditioning. We refer to these two groups as *freezers* and *darters* according to their respective dominant CS-evoked responses in early extinction.

One possible source of differences in behavioral responses to the CS during extinction could have been inter-group differences in fear conditioning or contextual fear generalization (from the conditioning box to the open field). However, no difference between groups was observed during fear acquisition (**Figure S2I**). Moreover, freezing levels were low during the ext1 baseline period prior to CS presentation, suggesting weak contextual fear, and were not significantly different between groups (**Figure S2J**). Another possible confound could be inter-group differences in within-day extinction learning. But, the difference in freezing levels between the last and the first CS presentations was not significantly different between the two groups (**Figure S2K**). As a control, the clustering analysis was performed with data from the last day of extinction, but this did not lead to groups with significant differences in behavior evolution over extinction (**Figure S1F-H**), indicating that interindividual differences in extinction behaviors were best captured by the phenotypes expressed in early extinction.

Like freezing, darting behavior increased after conditioning and decreased over extinction training in darters (**Figure 2G-H**). Moreover, darting was evoked by CS presentations (**Figure 2I-J**). These results are consistent with darting as an expression of conditioned defensive behavior specific for a subpopulation of the animals. Indeed, darting may be considered as an active behavioral pattern resembling flight and avoidance responses[9,10,18,19], since darting trajectories principally started and ended at sheltering locations in the arena (**Figure S2L-M**). Moreover, there was no significant difference in distance from sheltering locations between darters and freezers at CS onset (**Figure S2N**), ruling out the hypothesis that freezers darted less because they were already at sheltering locations then.

Behavioral phenotypes after fear conditioning predict differential levels of vulnerability to fear renewal

We then quantified fear renewal to test the hypothesis that post-conditioning behavioral profiles would predict context-dependent fear relapse. After 5 days of extinction in the open field, the animals were placed in a standard cubicle similar in size to those where initial conditioning took place, but different enough to be successfully discriminated,

since it evoked low contextual freezing (**Figure 3A**). As expected, CS presentation there elicited robust fear renewal in the form of high CS-triggered freezing relative to the end of extinction in both groups (**Figure S1A**). Surprisingly, here the CS triggered significantly more freezing in darters than in freezers (**Figure 3B**). This difference in fear renewal response strengths could not be accounted for by differences between groups in contextual fear levels or extinction rates during the renewal test (**Figure 3A**,**C**).

Complementing freezing measures, we quantified the magnitude of the orienting response displayed upon CS onset (**Video S2**) by measuring head movement. We took this as a proxy of the magnitude of the acoustic startle response, which is known to be potentiated by fear[20], since our setup was not suitable to measure the startle reflex itself. Orienting response magnitude was also greater in darters than freezers (**Figure 3D-E**), corroborating the result for freezing. Overall, the tendency of an animal to dart or to freeze after CS presentation during the first extinction session in the arena was, respectively, associated with higher or lower vulnerability to context-dependent fear renewal (**Figure 3F-I**).

Fear renewal vulnerability phenotypes are associated with different gene expression profiles

Finally, we sought to characterize specific biological substrates distinguishing these two behavioral phenotypes. Gene expression levels and their regulation have been associated with the recall and extinction of conditioned fear[21–24], as well as with Post-Traumatic Stress Disorder (PTSD)[25,26]. Therefore, we investigated whether the vulnerability phenotypes detected here were associated with distinct gene expression profiles. We assessed darters' and freezers' genome-wide transcriptional profiles in the ventromedial prefrontal cortex (vmPFC; **Figure 4A-B**), a region implicated in fear extinction, renewal, and PTSD[23,27–35].

Darters' and freezers' gene expression profiles clustered in two groups (**Figure 4C**), reflecting their behavioral phenotypes (**Figure 4D**), with 238 differentially expressed genes (DEGs; **Figures 4E**, **S3A**, **Table S1**). Among those, a gene ontology (GO) analysis revealed significantly enriched pathways comprising 49 genes which are involved in GABA signaling, regulation of membrane potential, membrane molecular organization, as well as glycogen catabolic processes (**Figure 4F**, **Table S2A**). In addition, we identified 45 DEGs involved in known protein-protein interaction (PPI) networks (**Figure S3B**, **Table S2B**). Finally, a disease-gene association (DGA) analysis revealed that 10 DEGs have previously been associated with PTSD, anxiety, or stress disorders[36,37] (**Figure S3C**, **Table S2C**).

In 22 cases, DEGs were highlighted by two or more of these analyses, marking them as possible key players in the vulnerability to fear relapse (**Figure S3D**, **Figure 4G**). Remarkably, these 22 genes were preferentially involved in synaptic functions and plasticity, and the expression of 19 of them was significantly correlated with the intensity of fear renewal (**Figure 4H**).

DISCUSSION

Here, we showed that behavioral markers emerging during early fear extinction predict interindividual differences in the intensity of fear renewal and associated cortical gene expression profiles in male rats. These behavioral markers and genes may represent targets for novel treatments to enhance context generalization of extinction training.

While freezing levels have been widely used as an index to study interindividual variability in fear behavior[9,38], to date they do not provide clear biomarkers of the vulnerability to fear relapse after recovery. Outside the laboratory, both humans and rodents can express multiple defensive behaviors in response to a perceived threat, such as freezing, fleeing, or attacking[39,40]. To improve the translation of findings from experiments with animal models to the clinic, one approach is to develop more naturalistic experiments to distinguish inter-individual responses by facilitating the expression and detection of a wider repertoire of behaviors[13–16]. Thus, we developed a new ethologically relevant paradigm combined with an automated pipeline for more extended behavioral profiling. This enabled the isolation of distinct behavioral phenotypes, including darting during early extinction which provided a marker of fear relapse vulnerability.

It is not possible to directly interpret our results in relation to previous work conducted in small enclosures. Indeed, in these settings, female rats display higher levels of darting[9,41–45], while other studies did not observe sex differences in active defensive responses[11,46]. The interindividual differences shown here may have led to the overall reduced incidence of darting responses detected in male rats in previous studies. The naturalistic environment here may also have contributed to revealing the darting responses that previous studies in smaller chambers did not elicit in male rats. Since trauma- and anxiety-related disorders have been reported as more prevalent in women[47,48], further investigations testing female rats with our paradigm may provide new and interesting translational perspectives.

The CS-evoked darting we observed in the large open field may be related to fear-related conditioned jumping previously observed in small conditioning chambers[9–11,41,46], which could well correspond to attempted escape responses. Consistent with this, in our results, darting was triggered by the CS onset, decreased with extinction training, and darting trajectories had the tendency to start and end in safer spots of the environment, all consistent with darting

as a CS-evoked defensive behavior. The transition between selecting darting or freezing may depend upon the characteristics and perceived level of safety of the current environment, or upon the physical and psychological distance from the perceived threat, as proposed by the predatory imminence theory[49,50], and confirmed by previous observations[e.g.51–53]. In this view, CS-evoked darting in the open field would be interpreted as a defensive response of animals perceiving the threat as being more imminent than it was perceived by the freezers. Interestingly, we showed that freezing, as an index of fear, does not transfer proportionally across environments. Perhaps, the darters expressed greater fear renewal in the form of freezing and orienting response because the constrained environment rendered their prevalent defense, darting, impossible. Future studies could explore this by testing renewal in environments allowing darting.

Understanding the biological mechanisms underlying interindividual responses to trauma and therapy is crucial for effective personalized therapy for patients. Here, we made a step towards deciphering the transcriptional coding landscape that is specifically associated with interindividual differences in vulnerability to fear renewal. We identified genes differentially expressed in more vs. less vulnerable subjects. Among others, these included genes involved in GABA signaling pathways, the regulation of membrane potential, and membrane proteic organization. These might be crucial for individual vulnerability to fear relapse by regulating long term synaptic plasticity mechanisms in the vmPFC, similarly to what has been reported in the amygdala for fear conditioning[54,55]. These genes could therefore correspond to interesting targets of future manipulative studies to test a potential direct role in fear relapse vulnerability. It must be noted that the transcriptional changes observed here may not be specific to the vmPFC. Also, it remains to be determined whether the biological pathways revealed here may play a causal role in interindividual levels of vulnerability. Future studies should focus on longitudinal analyses of changes in these regulatory pathways through conditioning, extinction, and renewal in order to better understand their respective roles in interindividual vulnerability levels.

Overall, our results challenge the tenet that assessment of freezing alone is sufficient to model post-traumatic behavior in rodents. This novel behavioral paradigm may be directly applied in translational research, since it directly identifies subjects vulnerable to fear renewal soon after the traumatic experience. To conclude, we showed here that a naturalistic environment can reveal the expression of an increased variety of defensive behaviors among laboratory animals and that post-conditioning behavioral phenotypes can serve as markers of the level of fear relapse vulnerability. These results may be instrumental for the development of more effective treatments enhancing context generalization of extinction training for psychiatric patients.

ACKNOWLEDGMENTS

We thank Matthieu Pasquet and Guillaume Dugué for help with inertial data acquisition and analysis, Karine Dias and Sophie Lemoine for RNA sequencing and raw transcriptomic data post-processing, Cédric Colas, Benjamin Billot, and Pierre-Antoine Vigneron for help with setting up of the apparatuses and protocols, and Valérie Doyère, Michaël Zugaro, and Gabrielle Girardeau for useful comments on the manuscript. This project was funded with grants from the Agence Nationale de la Recherche (ANR-12-SAMA-005) to BPG, TMJ, and SIW, Labex MemoLife (ANR-10-LABX-54 MEMO LIFE, ANR-10-IDEX-0001-02 PSL*) to MNP and SIW, Fondation Pierre Deniker to MNP, and Fondation de France (00081243 and 00091270) to M-OK. FD was supported by the Fondation pour la Recherche Medicale.

AUTHOR CONTRIBUTIONS

Research project conception and design: MNP, FD, BPG, TMJ. Funding gathering: BPG, TMJ, SIW, MNP, M-OK, FD. Technological implementation: MNP. Experiments: FD, MNP. Data analysis design: MNP, FD, RT, SIW, GM. Data analysis implementation: FD, MNP, RT, GM, AF. Visualization: MNP. Manuscript: MNP, FD, SIW, RT with comments from all authors. Project supervision and management: MNP.

DECLARATION OF INTERESTS

The authors declare no competing interests.

MAIN TEXT FIGURES LEGENDS

Figure 1. Multidimensional behavioral scoring in an ethologically-relevant paradigm reveals clusters of distinct post-conditioning fear response profiles.
(A) Behavioral protocol. Rats were habituated to forage in the arena containing sheltering objects (red shapes) for 5 days (hab1 to hab5), then underwent fear conditioning in a standard cubicle, followed by five days of extinction (ext1 to ext5) in the arena, and then by the fear renewal test (ren) in another cubicle.
(B) Automated multidimensional behavioral assessment tools.
(C) Example darting trajectory (thick colored line; triangle-start, circle-end). Gray traces: trajectories over 5 min.
(D) Darting peak speeds distribution (all trajectories, all rats).
(E) Fold change (FC) in behavioral variance compared to previous training stage (all behavioral classes, see STAR Methods). Solid line: mean; shading: SEM.
(F) PCs explained variance (green circles). Black line: shuffled data mean explained variance (shading: SEM). Stars: components with significant explained variance (Monte Carlo bootstrap).
(G) Behavioral classes' contributions to the significant PCs. Red: significant weights.
(H) Significant PCs expression during ext1 CS periods revealed two clusters. Dots: averages for each rat. Yellow and green: k-means separated clusters. Xs: cluster centers of mass; red dashed line: their Euclidean distance; red shaded areas: projections of contour lines of the Gaussian model's density estimates. Inset: inter-cluster distances distribution obtained for 1000 shuffles of group membership (red line: actual inter-cluster separation).
[***$p<0.001$]
See also Figures S1 and S2, and Video S1.

Figure 2. Distinct fear response profiles and their evolution over extinction training.
(A-B) Freezing and darting inter-group comparisons. Dots: averages across CSs for each rat. Box plots: central bar = median, bottom/top edges = 25th/75th percentiles; whiskers mark extreme points excluding outliers.
(C-E) After conditioning (D), darters and freezers formed two distinct clusters not distinguishable before conditioning (C) or after extinction (E). Similar format to Figure 1H.
(F) Darters-freezers cluster separation over time (red curve) compared to shuffled groups (gray line: mean; shading: 95% confidence interval). Red bars above: periods with significant separation (Monte Carlo bootstrap).
(G-H) Intra-group comparisons relative to extinction training (late habituation: hab4 and hab5; early extinction: ext1 and ext2; late extinction: ext4 and ext5).
(I-J) Locomotor speed around ext1 CSs presentations. Black dashed lines: CS onset and offset. (I) Individual trials. (J) Averages (solid lines) and SEM (shading). Gray bar: average baseline speed (20 s pre-CS). Bars above and below: periods significantly different from baseline.
[Sign-rank tests (A,B,G,H); Unpaired t-test (J); n.s.: not significant, *$p<0.05$, **$p<0.01$, ***$p<0.001$]
See also Figure S2.

Figure 3. Greater vulnerability to fear renewal in darters than freezers.
(A) Baseline freezing (prior to first CS).
(B) First CS period freezing.
(C) Freezing difference between first and last CS periods.
(D-E) Orienting responses measured from head angular velocity. (D) Individual trials, (E) average (solid lines) and SEM (shading). Inset: average response amplitude 0-500 ms.
(F-I) Fear renewal strength, measured as freezing (F-G) or orienting response (H-I) to the first CS, relative to ext1 freezing/darting. Same format and statistics as Figure 2.
[Unpaired t-tests (A,B,C,E); n.s.: not significant, *$p<0.05$, **$p<0.01$, ***$p<0.001$]
See also Video S2.

Figure 4. Darters and freezers have different gene expression profiles in vmPFC.
(A) Two n=7 groups were subsampled for transcriptomic analysis: same as Figure 3H, gray dots represent discarded data.
(B) Approximate location (blue circles) of the brain sampled for transcriptomic analysis (cingulate cortex areas 32V and 25).
(C) vmPFC transcriptomes PCA: PC1 and PC2 represented 32\% and 12\% of overall transcriptome variance.
(D) Linear regression analysis of gene expression profile (transcriptome PC1) vs. early extinction behavioral phenotypes.
(E) Scaled expression of DEGs for darters and freezers. Dendrograms: hierarchical clustering of individuals and genes according to gene expression. Only the 78 genes selected by the GO (panel F), PPI (Figure S3B), DGA (Figure S3C) analyses are labeled. Colored lettering: analyses for which the DEGs were retained.
(F) Significantly enriched Biological Processes Gene Ontology (GO) terms. Genes in bold typeface: identified in at least two among GO, PPI, and DGA analyses. Yellow/green: genes upregulated in freezers/darters.
(G) Summary of DEGs retained by at least two among GO, PPI, and DGA analyses. Node color intensity: gene relative expression in darters vs freezers. Lines: protein-protein associations.
(H) Correlation between gene expression and renewal freezing of DEGs retained in G. Circles color and size: correlation coefficient (Pearson, only those with $p<0.05$ are displayed.
See also Figure S3, and Tables S1-2.

STAR METHODS

RESOURCE AVAILABILITY

Lead contact

Further information and requests for resources should be directed to and will be fulfilled by the Lead Contact, Marco Pompili (marco.pompili@college-de-france.fr).

Materials availability

This study did not generate new unique reagents.

Data and code availability

Transcriptomic data are deposited on https://www.normalesup.org/~pompili while behavioral data are deposited on https://www.normalesup.org/~pompili. All original code has been deposited at https://www.normalesup.org/~pompili. DOIs are listed in the key resources table. Any additional information required to reanalyze the data reported in this paper is available from the lead contact upon request

EXPERIMENTAL MODEL AND SUBJECT DETAILS

18 adult male Long-Evans rats (260-340 g at the time of surgery, 2-4 months old), were housed in groups of 4 or 5 in large, environmentally-enriched, clear plastic cages (80x60x40cm) before surgery. They were maintained at 21°C in a well-ventilated room with a light/dark cycle of 12h/12h and free access to food and water. Upon arrival in the lab the animals were allowed at least 3 days of acclimatization before being handled daily by the experimenter for at least 5 days prior to surgery. All the experimental procedures were performed in accordance with institutional guidelines and national laws and policies, and were approved by the local Ethics Committee.

METHOD DETAILS

Surgical implantation of a magnetic base for the Inertial Measurements Unit (IMU)

The rats received a surgical implantation of a magnetic base onto which was fixed the Inertial Measurements Unit (IMU) during the experiments. The IMU is a small and lightweight device containing accelerometers and gyroscopes that sample linear acceleration and angular velocity of the animals' head in three dimensions[64]. The IMU was magnetically affixed to the animals' heads during the experiments. A pair of neodymium disk magnets (S-06-03-N, Supermagnete.com) was glued to the bottom face of the IMU, and another pair was cemented to the skull of the animals with a surgical procedure as described in[64]. Briefly, rats were anesthetized with an intraperitoneal injection of a mixture of ketamine (Imalgene, 180 mg/kg) and xylazine (Rompun, 10 mg/kg). Analgesia was assured by subcutaneous injection of buprenorphine (Buprecare, 0.025 mg/kg). The rats were placed in a stereotaxic frame (Narishige, Japan) and the surgical area was disinfected with povidone-iodine and 70% ethanol. The skull was exposed and gently scraped, and 3% hydrogen peroxide solution was applied. Burr holes were drilled (two in the frontal bone, five in the parietal bones, and one in the occipital bone) and miniature stainless steel screws (Phymep, France) were attached. Self-curing dental adhesive (Super-Bond C&B, Sun Medical) was deposited on the skull. A pair of disk neodymium magnets were glued to a glass/epoxy sheet and were fixed above the screws using self-curing acrylic resin (UNIFAST trad, GC Dental Products Corp.). The skin ridges were sutured in front and at the rear of the implant and the rats were allowed to recover in their home cages for one week. They then were housed individually in standard large cages (58x38x20 cm, DxHxW). After recovery. rats were placed under mild food restriction (~17 g/day, adjusted to allow for a 15 g weight gain per week until reaching 400 g, and then to maintain this weight) to ensure proper motivation for foraging during the sessions in the open field.

Behavioral protocol

After recovery from surgery, the rats underwent a 14 day ABC fear renewal protocol[65], which employed three different environments: two standard fear conditioning chambers (A and C) and one open field arena B. Auditory cues (CS) were 20 s continuous pure tones at 2 kHz (62-68 dB). Each day the rat had one training/testing session. Cameras mounted on the sides of the environments monitored animals' behaviors while a ceiling mounted video tracked their positions. During habituation (days 1 through 5), animals were habituated to the open field during 26 min sessions of free exploration and foraging. During fear conditioning (days 6 and 7), rats underwent two fear conditioning sessions in A, each composed of a 10 min baseline recording followed by five presentations of the CS each co-terminating with a footshock (1 s; 0.7 mA) at 10 minute intervals. Rats were then left undisturbed in their cages during days 8 and 9, during the weekend. Extinction: on days 10 to 13, rats underwent extinction training in B. Each session consisted of a 6-minute baseline recording followed by three presentations of the CS at intervals of 6 minutes. Fear renewal test: on day 15, all rats underwent a fear renewal test in C. After 6 min baseline recording, three CS were presented at 6 minute intervals.

Animals underwent 3 habituation sessions in B and 2 in B'. Half of the animals underwent extinction in B and the others in B'. On day 14, the last day of extinction, half of the animals in B were switched to B' and vice versa. No difference

in any of the behavioral measures was observed among animals who switched configuration on day 14 and those that did not, and their data were pooled.

Behavioral apparatus

The environment A was a transparent plexiglass box (37 x 45 x 37 cm, DxHxW) placed in a noise attenuating cubicle (Med Associates, USA). The floor consisted of 25 stainless steel rods (0.6 cm in diameter) connected to a constant-current scrambled shock generator (ENV-414, Med Associates, USA). C was a custom built PVC cubicle (40 x 40 x 40 cm) of dimensions similar to A, but with gray walls and a solid black floor. The open field could assume two different configurations, B and B', and was 250 x 150 cm with 70 cm high walls. While the walls and the floor were composed respectively of PVC and sheets of rubber in both B and B', the two configurations were different with respect to surface textures, distal cues visible in the room, and the identities of the objects (small models of Parisian and Roman monuments; $\sim$20x20x20cm each) within the open field. In B and B', to enhance the ethological relevance of the apparatus, we allowed foraging for food pellets (20 mg, MLabRodent Tablet, TestDiet) released from two ceiling-mounted automatic distributors (Camden Instruments, UK) every 20-40 s in each session. The conditioning and fear renewal test chambers were located in differently configured rooms on different floors of the same building.

In all environments, behavior was recorded from side-mounted cameras. In A and C, video was captured with a camcorder (Sony Handycam HDR-CX280) and, in B and B', with 4 video cameras (Basler Aca 2500-60) synchronized with Streampix 6 (Norpix, Canada). In B and B', video was also recorded at 30 Hz from above the open fields with a webcam (Logitech C920). The positions of red LEDs mounted on the IMU were tracked with Dacqtrack software (Axona, UK). Auditory cues (CS) were 20 s continuous pure tones at 2 kHz (62-68 dB) controlled by a Power1401 interface (CED, UK). This interface also controlled a flashing red LED (invisible to the animals) that helped synchronize position data acquisition.

Inertial signals acquisition and processing

The inertial measurement unit (IMU) is a small (19x13x13 mm) and lightweight (6 g) device[64]. The IMU employs Bluetooth wireless communication and the synchronization was assured by an infrared (IR) antenna that captured IR pulses emitted regularly at 0.5 Hz and recorded along with inertial data by the IMU. Sensitivity of the IMU was set to its maximum (±2 g and ±250°/s) and the sampling rate was 300 Hz. Preprocessing of inertial signals was performed with custom scripts in R. The head orientations were computed via low-pass filtering of all of the accelerometer signals[64]. A second-order Butterworth low-pass filter with a cut-off frequency of 2 Hz approximated gravity components.

Tissue sampling and genome sequencing

About 3 hours after the end of the renewal protocol, rats were anesthetized with isoflurane, then euthanized with a pentobarbital overdose (160 mg/kg, i.p.). Brains were immediately removed and frozen at -40°C in isopentane for 35 s and stored at -80°C until sectioning. Brains were sectioned (100µm) and the ventromedial prefrontal cortex (vmPFC) in sections from 4 to 2.7 mm rostral from bregma was micro-punched (0.75 mm punch diameter), bilaterally with a probe centered in the middle of the cingulate cortex areas 32 ventral and 25[66]. RNA was extracted using Trizol (Invitrogen) and further purified using the Direct-zolTM RNA MiniPrep (Zymo Research). Genome-wide transcriptional profiling was performed for seven rats in each group.

Genomewide transcriptional profiling was performed for seven rats in each group. Library preparation and Illumina sequencing were performed at the Ecole Normale Supérieure genomic core facility (Paris, France). Messenger (polyA+) RNAs were purified from 0.1 µg of total RNA using oligo(dT). Libraries were prepared using the strand specific RNA-Seq library preparation TruSeq Stranded mRNA kit (Illumina). Libraries were multiplexed by 14 on 4 high throughput flowcell lanes. A 75 bp single read sequencing was performed on a NextSeq 500 (Illumina). A mean of $2.298*10^7 \pm 3.189$ passing Illumina quality filter reads was obtained for each of the 14 samples.

Quantification and statistical analysis

Automatic scoring of behavior

All of the behavioral data presented in the figures result from an automated scoring pipeline.

Freezing was defined as each continuous period when the angular speed, computed from the IMU gyroscopes, was below 12°/s for at least 200 ms, as shown previously[64]. Since the animals were not equipped with the IMU during conditioning, freezing was manually scored for these sessions, and was defined as the absence of movement except for breathing. Object exploration was estimated as the time the animals spent within 5 cm around the objects. To detect **darting**, LED position data was smoothed with a 300 ms Gaussian window. Then, we first identified intervals when the animal moved at least 15 cm without changing direction (IMU-detected angular speed inferior to 3°/s in bins of 50 ms). The resulting straight trajectories were divided into darting vs. slower movement epochs by a k-means classification on the animal's speed.

A supervised deep learning algorithm scored the remaining behaviors. To create the training and test data sets, an experienced experimenter manually scored behaviors into the following categories: two types of grooming (face and body), rearing, freezing, and darting. The training and test sets were each derived from 98 minutes of video recordings from two extinction sessions for three randomly selected animals. **Grooming** was characterized by repetitive motion of the animals'

head, and of the forelimbs to its muzzle and whiskers (face grooming) or body (body grooming). **Rearing** was characterized as epochs when the animal was standing on its hind limbs. All other time bins were scored as '**foraging/exploratory**' and mostly included stationary activity, risk assessment, slow locomotion, and foraging behaviors.

A three-layer neural network with a convolutional layer and a fully connected hidden layer was implemented with custom scripts and built-in functions of the parallel computing toolbox in Matlab (Mathworks, USA). The behavioral measures provided to the network included: video-detected head position, accelerometer and gyroscope raw signals smoothed using a zero-phase lowpass filter, and the movement frequency power spectrum obtained by wavelet analysis of each gyroscope channel using the WaveletComp package in R that yielded a spectrogram of 3 bands, each 3 Hz wide, spanning from 0.1 to 9 Hz. All signals were down-sampled to 30 Hz and binned in 2 s windows with 200 ms overlap. Note that time bins previously classified as darting, freezing or object exploration (as defined above) were excluded from this analyses: the network thus only scored grooming, rearing vs. other behaviors. The network was trained on the manually scored behavior, and the robustness and accuracy of the classification was assessed on the test set by reiterating the training and test process 1000 times. The average accuracy of the classification was 87.7% (**Figure S4A**), consistent with previous reports[67]. The repeated iterations of the algorithm diverged by 3.8% on average and errors tended to be concentrated in the same 3.9% of bins (**Figure S4B-D**). Given the lack of differences between the different iterations, one iteration was randomly selected to classify the entire dataset.

Behavioral data analysis

Using all data over the course of the entire protocol for all sessions of all the animals, a six-column matrix containing the time series of the respective classified behaviors was built and smoothed (Gaussian window of 20 s). All of the CS and post-CS (60 s) data from the five extinction sessions of all of the animals was extracted and its dimensionality was reduced with Principal Component Analysis (PCA). Then, unsupervised clustering (k-means) separated the animals into two groups using the average activation strengths of the first three components of the PCA during the three CS presentations of the first extinction session (ext1). As a control, data was k-means clustered into two groups from data from the three CS presentations of the last session of extinction (ext5). Behavioral analyses were focused on CS evoked responses taking place in the intervals from CS onsets until 60 seconds after CS offsets, here named CS periods.

The clustering and all statistical analyses were performed in Matlab (MathWorks, Natick, MA), using the Freely Moving Animal Toolbox (http://fmatoolbox.sourceforge.net) and custom written programs. Behavioral categories whose weights exceeded Otsu's threshold[68] were considered as significantly contributing to the corresponding principal component. Otsu's threshold selection is a nonparametric and unsupervised method to set a threshold to extract relevant values from background activity.

In figure 3J, to increase the temporal resolution of behavioral cluster separation analysis we separated CS from post-CS in order to represent each session by 6 different intervals. For descriptive statistics, behavioral data was represented with boxplots where the central bar indicates the median, the bottom and top edges indicate the 25th and 75th percentiles; whiskers extend to the most extreme data points, excluding outliers. Datapoints were considered as outliers if they were greater than $q3+2.7\sigma(q3 - q1)$ or less than $q1-2.7\sigma(q3 - q1)$; where σ is the standard deviation, and q1 and q3 are, respectively, the 25th and 75th percentiles of the sample data. To represent overall changes in behavioral variance across the protocol (Figure 1E), the values of variance for the different behavioral classes (Figure S1A) for each day were pooled and fold change was computed relative to the average value of the previous day. Training stages were defined as in Figure 2G-H but early habituation only included hab2 since FC compared to previous day cannot be computed for hab1.

Differentially expressed genes analysis

The analyses of sequenced data were performed using the Eoulsan pipeline[56], including read filtering, mapping, alignment filtering, read quantification, normalisation and differential analysis. Before mapping, poly N read tails were trimmed, reads <40 bases were removed, and reads with quality mean < 30 were discarded. Reads were then aligned against the Rattus norvegicus genome from Ensembl version 96 using STAR (version 2.7.2d)[58]. Alignments from reads matching more than once on the reference genome were removed using Java version of samtools[57]. To compute gene expression, Rattus norvegicus GTF genome annotation version 96 from Ensembl database was used. All overlapping regions between alignments and referenced exons were counted using HTSeq-count 0.5.3[59]. The sample counts were normalized using DESeq2 1.8.1[60]. Statistical treatments and differential analyses were also performed using DESeq2 1.8.1.

Transcriptomics data analysis was performed using routines written in R. Differentially expressed genes (DEGs) were defined by an absolute value of log2 of fold change >1, an adjusted p-values after Bejamini & Hochberg correction[69] of <0.01, and mean total counts for all the conditions >10. In order to assure stringent selection, further correction was performed non-parametrically with a shuffling technique. We randomly permuted 3431 times (for all possible combinations of two groups of 7 subjects) the assignment of BH corrected p-values to the two groups. For each gene, we computed the number of times the difference in gene expression between the two groups in shuffled data was equal or greater than the difference observed. This was <0.02 in all cases, and we therefore retained all DEGs. Volcano plots and heatmaps for visualization were generated using the Enhanced Volcano (https://bioconductor.org/packages/devel/bioc/vignettes/EnhancedVolcano/inst/doc/EnhancedVolcano.html) and Complex Heatmap[70] R packages.

Gene annotation and enrichment analysis on the 238 DEGs was performed using Metascape with a minimum count of 5 and default parameters otherwise (http://metascape.org/)[61]. All genes in the genome have been used as the enrichment background. Among the DEGs, 190 genes were detected in the ontology sources GO Biological Processes. P-values were calculated based on the accumulative hypergeometric distribution, and q-values were calculated using the Benjamini-Hochberg procedure to account for multiple testing. Protein-protein interactions analysis between the DEGs was performed using STRING (Search Tool for Recurring Instances of Neighboring Genes, v 11.0 (https://string-db.org/)[62]. Interaction sources include all sources available in STRING. Disconnected nodes are not displayed in Figures. Minimum required interaction score was set to a high confidence level (0.7). Disease Gene association between the DEGs and the stress and anxiety related disorders ("Post-Traumatic Stress Disorder", "Anxiety Disorders", "Anxiety symptoms", "Anxiety", "Anxiety and fear", "Abnormal fear/anxiety-related behavior", "Stress, Psychological") was performed using the DisGeNET database[63].

SUPPLEMENTAL VIDEOS LEGENDS

Video S1. Examples of the 6 behavioral categories. Relates to Figure 1.
The video is provided as a separate file.

Video S2. Example of a CS-evoked orienting response and associated startling in a small compartment. Relates to Figure 3.
The video is provided as a separate file.

REFERENCES

1. Hoskins, M., Pearce, J., Bethell, A., Dankova, L., Barbui, C., Tol, W.A., Van Ommeren, M., De Jong, J., Seedat, S., and Chen, H. (2015). Pharmacotherapy for post-traumatic stress disorder: systematic review and meta-analysis. Br. J. Psychiatry *206*, 93–100. 10.1192/bjp.bp.114.148551.
2. Cusack, K., Jonas, D.E., Forneris, C.A., Wines, C., Sonis, J., Middleton, J.C., Feltner, C., Brownley, K.A., Olmsted, K.R., and Greenblatt, A. (2016). Psychological treatments for adults with posttraumatic stress disorder: A systematic review and meta-analysis. Clin. Psychol. Rev. *43*, 128–141. 10.1016/j.cpr.2015.10.003.
3. Mary, A., Dayan, J., Leone, G., Postel, C., Fraisse, F., Malle, C., Vallée, T., Klein-Peschanski, C., Viader, F., and De la Sayette, V. (2020). Resilience after trauma: The role of memory suppression. Science (80-.). *367*, eaay8477. 10.1126/science.aay8477.
4. Milad, M.R., Pitman, R.K., Ellis, C.B., Gold, A.L., Shin, L.M., Lasko, N.B., Zeidan, M.A., Handwerger, K., Orr, S.P., and Rauch, S.L. (2009). Neurobiological basis of failure to recall extinction memory in posttraumatic stress disorder. Biol. Psychiatry *66*, 1075–1082. 10.1016/j.biopsych.2009.06.026.
5. Powers, M.B., Halpern, J.M., Ferenschak, M.P., Gillihan, S.J., and Foa, E.B. (2010). A meta-analytic review of prolonged exposure for posttraumatic stress disorder. Clin. Psychol. Rev. *30*, 635–641. 10.1016/j.cpr.2010.04.007.
6. Etkin, A., Maron-Katz, A., Wu, W., Fonzo, G.A., Huemer, J., Vértes, P.E., Patenaude, B., Richiardi, J., Goodkind, M.S., and Keller, C.J. (2019). Using fMRI connectivity to define a treatment-resistant form of post-traumatic stress disorder. Sci. Transl. Med. *11*, eaal3236. 10.1126/scitranslmed.aal3236.
7. Zhutovsky, P., Thomas, R.M., Olff, M., van Rooij, S.J.H., Kennis, M., van Wingen, G.A., and Geuze, E. (2019). Individual prediction of psychotherapy outcome in posttraumatic stress disorder using neuroimaging data. Transl. Psychiatry *9*, 326. 10.1038/s41398-019-0663-7.
8. Korgaonkar, M.S., Chakouch, C., Breukelaar, I.A., Erlinger, M., Felmingham, K.L., Forbes, D., Williams, L.M., and Bryant, R.A. (2020). Intrinsic connectomes underlying response to trauma-focused psychotherapy in post-traumatic stress disorder. Transl. Psychiatry *10*, 270. 10.1038/s41398-020-00938-8.
9. Gruene, T.M., Flick, K., Stefano, A., Shea, S.D., and Shansky, R.M. (2015). Sexually divergent expression of active and passive conditioned fear responses in rats. Elife *4*, e11352. 10.7554/elife.11352.
10. Fadok, J.P., Krabbe, S., Markovic, M., Courtin, J., Xu, C., Massi, L., Botta, P., Bylund, K., Müller, C., Kovacevic, A., et al. (2017). A competitive inhibitory circuit for selection of active and passive fear responses. Nature *542*, 96. 10.1038/nature21047.
11. Totty, M.S., Warren, N., Huddleston, I., Ramanathan, K.R., Ressler, R.L., Oleksiak, C.R., and Maren, S. (2021). Behavioral and brain mechanisms mediating conditioned flight behavior in rats. Sci. Rep. *11*, 1–15. 10.1038/s41598-021-87559-3.
12. Krakauer, J.W., Ghazanfar, A.A., Gomez-Marin, A., MacIver, M.A., and Poeppel, D. (2017). Neuroscience needs behavior: correcting a reductionist bias. Neuron *93*, 480–490. 10.1016/j.neuron.2016.12.041.
13. Mobbs, D., and Kim, J.J. (2015). Neuroethological studies of fear, anxiety, and risky decision-making in rodents and humans. Curr. Opin. Behav. Sci. *5*, 8–15. 10.1016/j.cobeha.2015.06.005.
14. Paré, D., and Quirk, G.J. (2017). When scientific paradigms lead to tunnel vision: lessons from the study of fear. Sci. Learn. *2*, 1–8. 10.1038/s41539-017-0007-4.
15. Kim, J.J., and Jung, M.W. (2018). Fear paradigms: The times they are a-changin'. Curr. Opin. Behav. Sci. *24*, 38–43. 10.1016/j.cobeha.2018.02.007.

16. Headley, D.B., Kanta, V., Kyriazi, P., and Paré, D. (2019). Embracing Complexity in Defensive Networks. Neuron *103*, 189–201. 10.1016/j.neuron.2019.05.024.
17. Reinhold, A.S., Sanguinetti-Scheck, J.I., Hartmann, K., and Brecht, M. (2019). Behavioral and neural correlates of hide-and-seek in rats. Science (80-.). *365*, 1180–1183. 10.1126/science.aax4705.
18. Choi, J.-S., and Kim, J.J. (2010). Amygdala regulates risk of predation in rats foraging in a dynamic fear environment. Proc. Natl. Acad. Sci. U. S. A. *107*, 21773–21777. https://doi.org/10.1073/pnas.1010079108.
19. Kyriazi, P., Headley, D.B., and Pare, D. (2018). Multi-dimensional Coding by Basolateral Amygdala Article Multi-dimensional Coding by Basolateral Amygdala Neurons. Neuron *99*, 1315–1328. 10.1016/j.neuron.2018.07.036.
20. Davis, M., Falls, W.A., Campeau, S., and Kim, M. (1993). Fear-potentiated startle: a neural and pharmacological analysis. Behav. Brain Res. *58*, 175–198. 10.1016/0166-4328(93)90102-v.
21. Soliman, F., Glatt, C.E., Bath, K.G., Levita, L., Jones, R.M., Pattwell, S.S., Jing, D., Tottenham, N., Amso, D., and Somerville, L.H. (2010). A genetic variant BDNF polymorphism alters extinction learning in both mouse and human. Science (80-.). *327*, 863–866. 10.1126/science.1181886.
22. Lin, Q., Wei, W., Coelho, C.M., Li, X., Baker-Andresen, D., Dudley, K., Ratnu, V.S., Boskovic, Z., Kobor, M.S., and Sun, Y.E. (2011). The brain-specific microRNA miR-128b regulates the formation of fear-extinction memory. Nat. Neurosci. *14*, 1115–7. 10.1038/nn.2891.
23. Stafford, J.M., Raybuck, J.D., Ryabinin, A.E., and Lattal, K.M. (2012). Increasing histone acetylation in the hippocampus-infralimbic network enhances fear extinction. Biol. Psychiatry *72*, 25–33. 10.1016/j.biopsych.2011.12.012.
24. Li, X., Zhao, Q., Wei, W., Lin, Q., Magnan, C., Emami, M.R., Wearick-Silva, L.E., Viola, T.W., Marshall, P.R., and Yin, J. (2019). The DNA modification N6-methyl-2'-deoxyadenosine (m6dA) drives activity-induced gene expression and is required for fear extinction. Nat. Neurosci. *22*, 534–544. 10.1038/s41593-019-0339-x.
25. Ressler, K.J., Mercer, K.B., Bradley, B., Jovanovic, T., Mahan, A., Kerley, K., Norrholm, S.D., Kilaru, V., Smith, A.K., Myers, A.J., et al. (2011). Post-traumatic stress disorder is associated with PACAP and the PAC1 receptor. Nature *470*, 492–497. 10.1038/nature09856.
26. Breen, M.S., Tylee, D.S., Maihofer, A.X., Neylan, T.C., Mehta, D., Binder, E.B., Chandler, S.D., Hess, J.L., Kremen, W.S., Risbrough, V.B., et al. (2018). PTSD Blood Transcriptome Mega-Analysis: Shared Inflammatory Pathways across Biological Sex and Modes of Trauma. Neuropsychopharmacology *43*, 469–481. 10.1038/npp.2017.220.
27. Milad, M.R., and Quirk, G.J. (2002). Neurons in medial prefrontal cortex signal memory for fear extinction. Nature *420*, 70–74. 10.1038/nature01138.
28. Kalisch, R., Korenfeld, E., Stephan, K.E., Weiskopf, N., Seymour, B., and Dolan, R.J. (2006). Context-dependent human extinction memory is mediated by a ventromedial prefrontal and hippocampal network. J. Neurosci. *26*, 9503–9511. 10.1523/JNEUROSCI.2021-06.2006.
29. Milad, M.R., Wright, C.I., Orr, S.P., Pitman, R.K., Quirk, G.J., and Rauch, S.L. (2007). Recall of fear extinction in humans activates the ventromedial prefrontal cortex and hippocampus in concert. Biol. Psychiatry *62*, 446–54. 10.1016/j.biopsych.2006.10.011.
30. Peters, J., Dieppa-Perea, L.M., Melendez, L.M., and Quirk, G.J. (2010). Induction of fear extinction with hippocampal-infralimbic BDNF. Science (80-.). *328*, 1288–1290. 10.1126/science.1186909.
31. Sierra-Mercado, D., Padilla-Coreano, N., and Quirk, G.J. (2011). Dissociable roles of prelimbic and infralimbic cortices, ventral hippocampus, and basolateral amygdala in the expression and extinction of conditioned fear. Neuropsychopharmacology *36*, 529–538. 10.1038/npp.2010.184.
32. Knapska, E., Macias, M., Mikosz, M., Nowak, A., Owczarek, D., Wawrzyniak, M., Pieprzyk, M., Cymerman, I. a, Werka, T., Sheng, M., et al. (2012). Functional anatomy of neural circuits regulating fear and extinction. Proc. Natl. Acad. Sci. U. S. A. *109*, 17093–8. 10.1073/pnas.1202087109.
33. Garfinkel, S.N., Abelson, J.L., King, A.P., Sripada, R.K., Wang, X., Gaines, L.M., and Liberzon, I. (2014). Impaired contextual modulation of memories in PTSD: an fMRI and psychophysiological study of extinction retention and fear renewal. J. Neurosci. *34*, 13435–13443. 10.1523/jneurosci.4287-13.2014.
34. Do-Monte, F.H., Quiñones-Laracuente, K., Quirk, G.J., Quinõnes-Laracuente, K., Quirk, G.J., Quiñones-Laracuente, K., Quirk, G.J., Quinõnes-Laracuente, K., and Quirk, G.J. (2015). A temporal shift in the circuits mediating retrieval of fear memory. Nature *519*, 460–463. 10.1038/nature14030.
35. Marek, R., Jin, J., Goode, T.D., Giustino, T.F., Wang, Q., Acca, G.M., Holehonnur, R., Ploski, J.E., Fitzgerald, P.J., Lynagh, T., et al. (2018). Hippocampus-driven feed-forward inhibition of the prefrontal cortex mediates relapse of extinguished fear. Nat. Neurosci. *21*, 384. 10.1038/s41593-018-0073-9.
36. Roberts, J.E., Tonnsen, B.L., McCary, L.M., Ford, A.L., Golden, R.N., and Bailey Jr, D.B. (2016). Trajectory and predictors of depression and anxiety disorders in mothers with the FMR1 premutation. Biol. Psychiatry *79*, 850–857. 10.1016/j.biopsych.2015.07.015.
37. Meier, S.M., Trontti, K., Purves, K.L., Als, T.D., Grove, J., Laine, M., Pedersen, M.G., Bybjerg-Grauholm, J., Bækved-Hansen, M., and Sokolowska, E. (2019). Genetic variants associated with anxiety and stress-related disorders: a genome-wide association study and mouse-model study. JAMA Psychiatry *76*, 924–932. 10.1001/jamapsychiatry.2019.1119.
38. Dopfel, D., Perez, P.D., Verbitsky, A., Bravo-Rivera, H., Ma, Y., Quirk, G.J., and Zhang, N. (2019). Individual variability in behavior and functional networks predicts vulnerability using an animal model of PTSD. Nat. Commun. *10*, 2372. 10.1038/s41467-019-09926-z.
39. LeDoux, J.E., and Daw, N.D. (2018). Surviving threats: Neural circuit and computational implications of a new taxonomy of defensive behaviour. Nat. Rev. Neurosci. *19*, 269–282. 10.1038/nrn.2018.22.
40. Fanselow, M.S. (2018). Emotion, motivation and function. Curr. Opin. Behav. Sci. *19*, 105–109. 10.1016/j.cobeha.2017.12.013.
41. Pellman, B.A., Schuessler, B.P., Tellakat, M., and Kim, J.J. (2017). Sexually dimorphic risk mitigation strategies in rats. eNeuro *4*, 1–11. 10.1523/ENEURO.0288-16.2017.
42. Colom-Lapetina, J., Li, A.J., Pelegrina-Perez, T.C., and Shansky, R.M. (2019). Behavioral diversity across classic rodent models is sex-dependent. Front. Behav. Neurosci. *13*, 1–8. 10.3389/fnbeh.2019.00045.

43. Greiner, E.M., Müller, I., Norris, M.R., Ng, K.H., and Sangha, S. (2019). Sex differences in fear regulation and reward-seeking behaviors in a fear-safety-reward discrimination task. Behav. Brain Res. *368*. 10.1016/j.bbr.2019.111903.
44. Mitchell, J.R., Trettel, S.G., Li, A.J., Wasielewski, S., Huckleberry, K.A., Fanikos, M., Golden, E., and Shansky, R.M. (2021). Parametric modulators of sex-biased conditioned fear responding. Prepr. bioRxiv. 10.1101/2021.06.30.450556.
45. Morena, M., Nastase, A.S., Santori, A., Cravatt, B.F., Shansky, R.M., and Hill, M.N. (2021). Sex-dependent effects of endocannabinoid modulation of conditioned fear extinction in rats. Br. J. Pharmacol. *178*, 983–996. 10.1111/bph.15341.
46. Borkar, C.D., Dorofeikova, M., Le, Q.S.E., Vutukuri, R., Vo, C., Hereford, D., Resendez, A., Basavanhalli, S., Sifnugel, N., and Fadok, J.P. (2020). Sex differences in behavioral responses during a conditioned flight paradigm. Behav. Brain Res. *389*, 112623. 10.1016/j.bbr.2020.112623.
47. Kessler, R.C., Sonnega, A., Bromet, E., Hughes, M., and Nelson, C.B. (1995). Posttraumatic stress disorder in the national comorbidity survey. Arch. Gen. Psychiatry *52*, 1048–1060. 10.1001/archpsyc.1995.03950240066012.
48. McLean, C.P., Asnaani, A., Litz, B.T., and Hofmann, S.G. (2011). Gender differences in anxiety disorders: Prevalence, course of illness, comorbidity and burden of illness. J. Psychiatr. Res. *45*, 1027–1035. 10.1016/j.jpsychires.2011.03.006.
49. Blanchard, R.J., Flannelly, K.J., and Blanchard, D.C. (1986). Defensive behavior of laboratory and wild Rattus norvegicus. J. Comp. Psychol. *100*, 101–107. 10.1037/0735-7036.100.2.101.
50. Fanselow, M.S., and Lester, L.S. (1988). A functional behavioristic approach to aversively motivated behavior: Predatory imminence as a determinant of the topography of defensive behavior. In Evolution and Learning, R. C. Bolles and M. D. Beecher, eds. (Lawrence Erlbaum Associates, Inc), pp. 185–212.
51. Yilmaz, M., and Meister, M. (2013). Rapid innate defensive responses of mice to looming visual stimuli. Curr. Biol. *23*, 2011–2015. 10.1016/j.cub.2013.08.015.
52. Salay, L.D., Ishiko, N., and Huberman, A.D. (2018). A midline thalamic circuit determines reactions to visual threat. Nature *557*, 183–189. 10.1038/s41586-018-0078-2.
53. Evans, D.A., Stempel, V.A., Vale, R., Ruehle, S., Lefler, Y., and Branco, T. (2018). A synaptic threshold mechanism for computing escape decisions. Nature *558*, 590–594. 10.1057/9780230234208_3.
54. Shaban, H., Humeau, Y., Herry, C., Cassasus, G., Shigemoto, R., Ciocchi, S., Barbieri, S., Van Der Putten, H., Kaupmann, K., and Bettler, B. (2006). Generalization of amygdala LTP and conditioned fear in the absence of presynaptic inhibition. Nat. Neurosci. *9*, 1028–1035. 10.1038/nn1732.
55. Lange, M.D., Jüngling, K., Paulukat, L., Vieler, M., Gaburro, S., Sosulina, L., Blaesse, P., Sreepathi, H.K., Ferraguti, F., and Pape, H.-C. (2014). Glutamic acid decarboxylase 65: a link between GABAergic synaptic plasticity in the lateral amygdala and conditioned fear generalization. Neuropsychopharmacology *39*, 2211–2220. 10.1038/npp.2014.72.
56. Jourdren, L., Bernard, M., Dillies, M.-A., and Le Crom, S. (2012). Eoulsan: a cloud computing-based framework facilitating high throughput sequencing analyses. Bioinformatics *28*, 1542–1543. 10.1093/bioinformatics/bts165.
57. Li, H., Handsaker, B., Wysoker, A., Fennell, T., Ruan, J., Homer, N., Marth, G., Abecasis, G., and Durbin, R. (2009). The sequence alignment/map format and SAMtools. Bioinformatics *25*, 2078–2079. 10.1093/bioinformatics/btp352.
58. Dobin, A., Davis, C.A., Schlesinger, F., Drenkow, J., Zaleski, C., Jha, S., Batut, P., Chaisson, M., and Gingeras, T.R. (2013). STAR: ultrafast universal RNA-seq aligner. Bioinformatics *29*, 15–21. 10.1093/bioinformatics/bts635.
59. Anders, S., Pyl, P.T., and Huber, W. (2015). HTSeq—a Python framework to work with high-throughput sequencing data. Bioinformatics *31*, 166–169. 10.1093/bioinformatics/btu638.
60. Love, M.I., Huber, W., and Anders, S. (2014). Moderated estimation of fold change and dispersion for RNA-seq data with DESeq2. Genome Biol. *15*, 550. 10.1186/s13059-014-0550-8.
61. Zhou, Y., Zhou, B., Pache, L., Chang, M., Khodabakhshi, A.H., Tanaseichuk, O., Benner, C., and Chanda, S.K. (2019). Metascape provides a biologist-oriented resource for the analysis of systems-level datasets. Nat. Commun. *10*, 1–10. 10.1038/s41467-019-09234-6.
62. Szklarczyk, D., Morris, J.H., Cook, H., Kuhn, M., Wyder, S., Simonovic, M., Santos, A., Doncheva, N.T., Roth, A., and Bork, P. (2016). The STRING database in 2017: quality-controlled protein–protein association networks, made broadly accessible. Nucleic Acids Res., gkw937. 10.1093/nar/gkw937.
63. Piñero, J., Ramírez-Anguita, J.M., Saüch-Pitarch, J., Ronzano, F., Centeno, E., Sanz, F., and Furlong, L.I. (2020). The DisGeNET knowledge platform for disease genomics: 2019 update. Nucleic Acids Res. *48*, D845–D855. 10.1093/nar/gkz1021.
64. Pasquet, M.O., Tihy, M., Gourgeon, A., Pompili, M.N., Godsil, B.P., Lena, C., Dugué, G.P., Léna, C., Dugué, G.P., Lena, C., et al. (2016). Wireless inertial measurement of head kinematics in freely-moving rats. Sci. Rep. *6*, 1–18. 10.1038/srep35689.
65. Bouton, M.E. (2004). Context and behavioral processes in extinction. Learn. Mem. *11*, 485–494. 10.1101/lm.78804.
66. Paxinos, G., and Watson, C. (2013). The Rat Brain in Stereotaxic Coordinates - 7th edition (Academic Press).
67. Venkatraman, S., Jin, X., Costa, R.M., and Carmena, J.M. (2010). Investigating neural correlates of behavior in freely behaving rodents using inertial sensors. J. Neurophysiol. *104*, 569–575. 10.1152/jn.00121.2010.
68. Otsu, N. (1979). A threshold selection method from gray-level histograms. IEEE Trans. Syst. Man. Cybern. *9*, 62–66. 10.1109/TSMC.1979.4310076.
69. Benjamini, Y., and Hochberg, Y. (1995). Controlling the false discovery rate: a practical and powerful approach to multiple testing. J. R. Stat. Soc. Ser. B *57*, 289–300. 10.1111/j.2517-6161.1995.tb02031.x.
70. Gu, Z., Eils, R., and Schlesner, M. (2016). Complex heatmaps reveal patterns and correlations in multidimensional genomic data. Bioinformatics *32*, 2847–2849. 10.1093/bioinformatics/btw313.

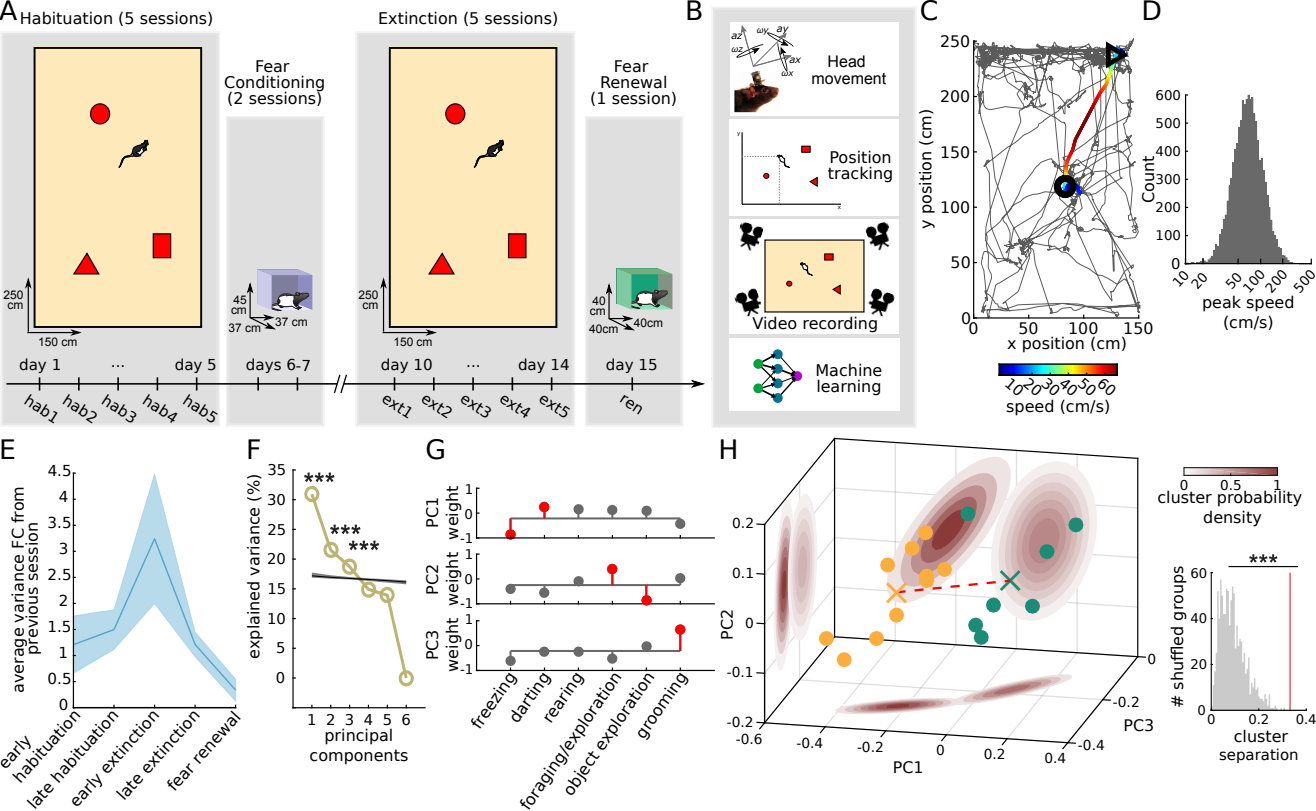
A
Habituation (5 sessions)
Fear Conditioning (2 sessions)
Extinction (5 sessions)
Fear Renewal (1 session)
250 cm
150 cm
45 cm
37 cm
37 cm
40 cm
40cm
40cm
day 1
...
day 5
days 6-7
day 10
...
day 14
day 15
hab1
hab2
hab3
hab4
hab5
ext1
ext2
ext3
ext4
ext5
ren
B
Head movement
Position tracking
Video recording
Machine learning
C
y position (cm)
x position (cm)
speed (cm/s)
D
Count
peak speed (cm/s)
E
average variance FC from previous session
early habituation
late habituation
early extinction
late extinction
fear renewal
F
explained variance (%)
principal components
G
PC1 weight
PC2 weight
PC3 weight
freezing
darting
rearing
foraging/exploration
object exploration
grooming
H
PC1
PC2
PC3
cluster probability density
shuffled groups
cluster separation

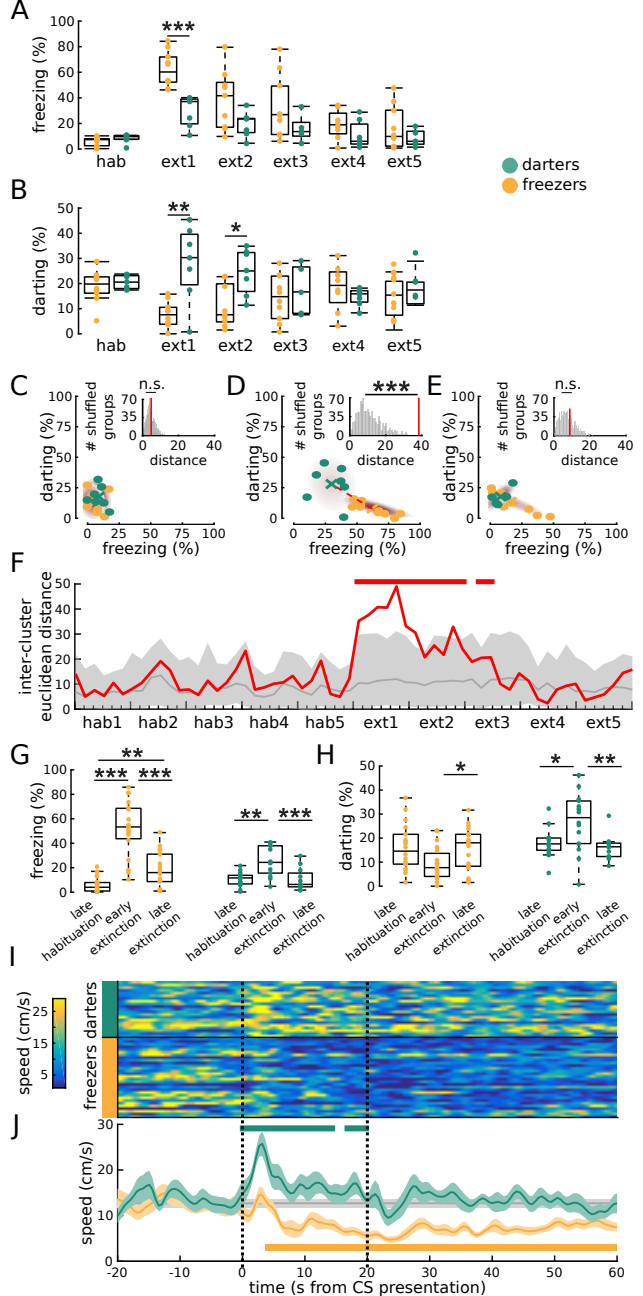
A
freezing (%)
***
hab
ext1
ext2
ext3
ext4
ext5
darters
freezers
B
darting (%)
**
*
C
D
E
n.s.
***
shuffled groups
distance
darting (%)
freezing (%)
F
inter-cluster euclidean distance
hab1
hab2
hab3
hab4
hab5
G
late habituation
early extinction
late extinction
H
I
speed (cm/s)
freezers
darters
J
time (s from CS presentation)

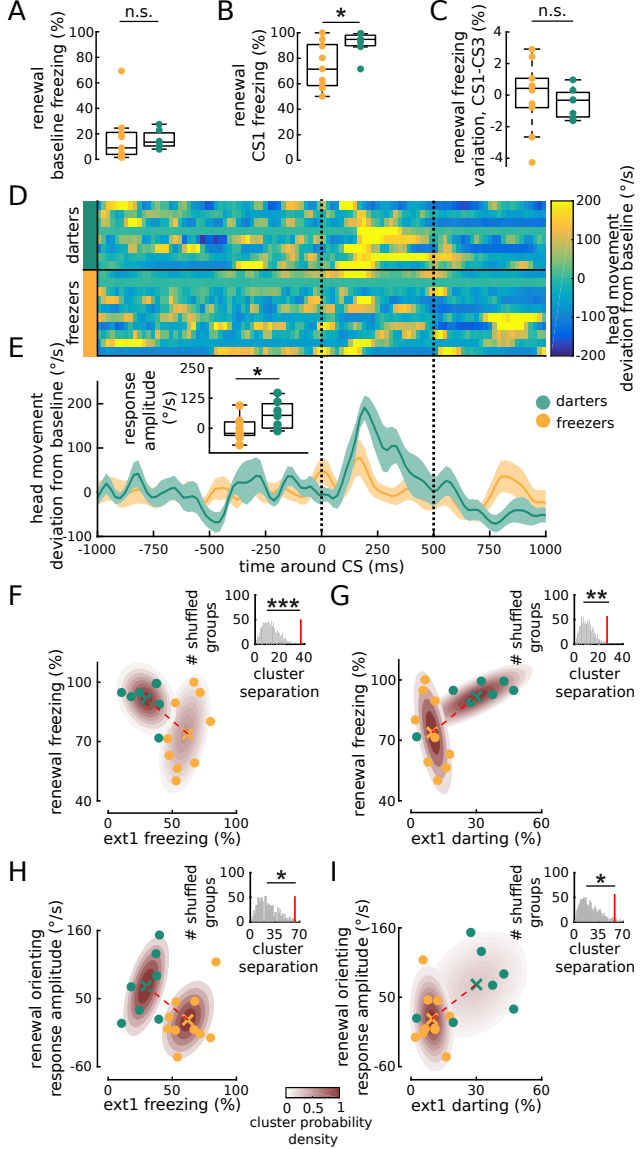
A
n.s.
renewal baseline freezing (%)
B
*
renewal CS1 freezing (%)
C
n.s.
renewal freezing variation, CS1-CS3 (%)
D
darters
freezers
head movement deviation from baseline (°/s)
E
head movement deviation from baseline (°/s)
response amplitude (°/s)
*
darters
freezers
time around CS (ms)
F
renewal freezing (%)
ext1 freezing (%)
shuffled groups
***
cluster separation
G
renewal freezing (%)
ext1 darting (%)
shuffled groups
**
cluster separation
H
renewal orienting response amplitude (°/s)
ext1 freezing (%)
shuffled groups
*
cluster separation
cluster probability density
I
renewal orienting response amplitude (°/s)
ext1 darting (%)
shuffled groups
*
cluster separation

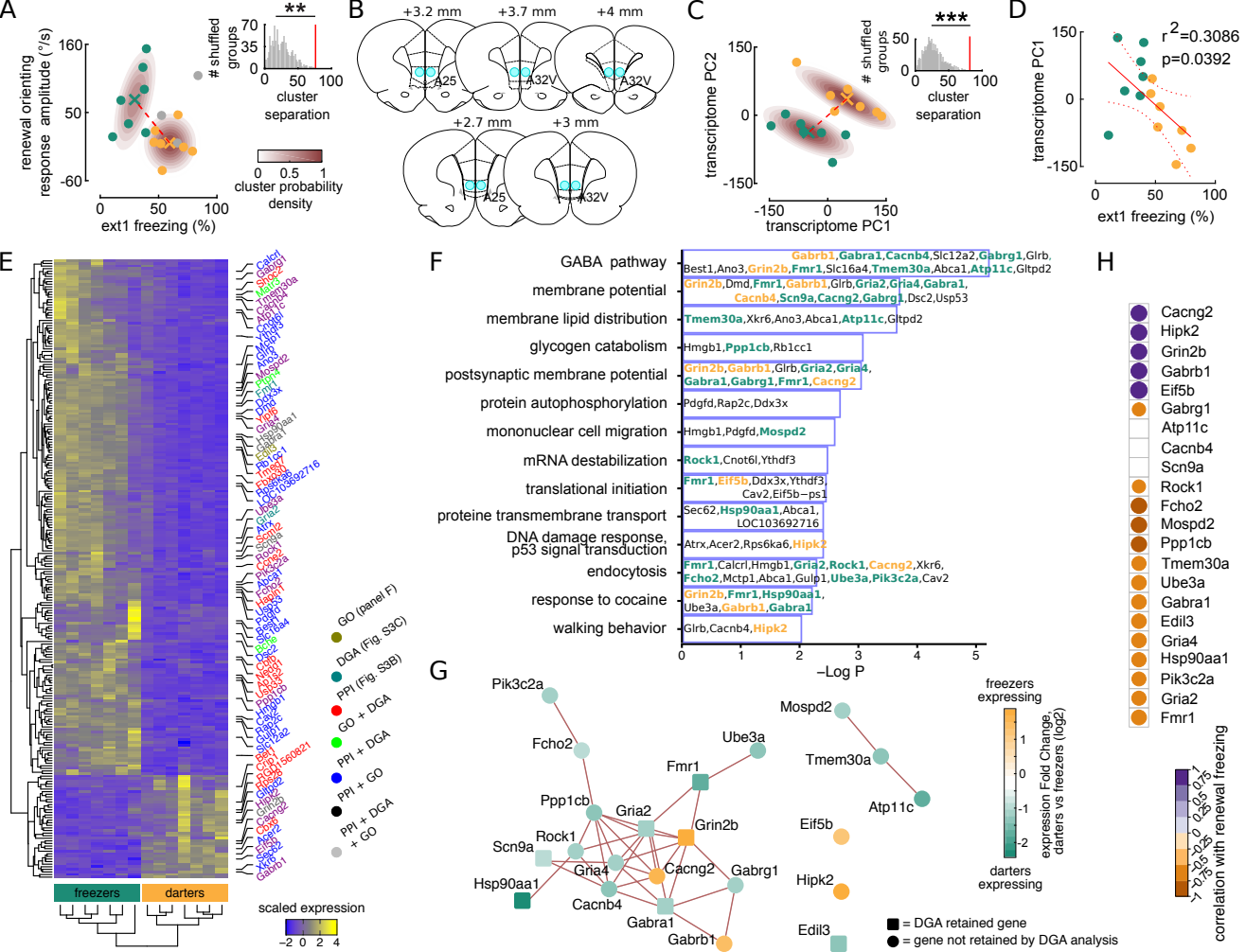
A
renewal orienting response amplitude (°/s)
ext1 freezing (%)
shuffled groups
cluster separation
cluster probability density
B
+3.2 mm
+3.7 mm
+4 mm
+2.7 mm
+3 mm
A25
A32V
C
transcriptome PC2
transcriptome PC1
D
r2=0.3086
p=0.0392
transcriptome PC1
ext1 freezing (%)
E
freezers
darters
scaled expression
GO (panel F)
DGA (Fig. S3C)
PPI (Fig. S3B)
GO + DGA
PPI + DGA
PPI + GO
PPI + DGA + GO
F
GABA pathway
membrane potential
membrane lipid distribution
glycogen catabolism
postsynaptic membrane potential
protein autophosphorylation
mononuclear cell migration
mRNA destabilization
translational initiation
proteine transmembrane transport
DNA damage response, p53 signal transduction
endocytosis
response to cocaine
walking behavior
−Log P
G
Pik3c2a
Fcho2
Ube3a
Fmr1
Ppp1cb
Gria2
Grin2b
Rock1
Scn9a
Gria4
Cacng2
Gabrg1
Hsp90aa1
Cacnb4
Gabra1
Gabrb1
Mospd2
Tmem30a
Atp11c
Eif5b
Hipk2
Edil3
freezers expressing
darters expressing
expression Fold Change darters vs freezers (log2)
= DGA retained gene
= gene not retained by DGA analysis
H
Cacng2
Hipk2
Grin2b
Gabrb1
Eif5b
Gabrg1
Atp11c
Cacnb4
Scn9a
Rock1
Fcho2
Mospd2
Ppp1cb
Tmem30a
Ube3a
Gabra1
Edil3
Gria4
Hsp90aa1
Pik3c2a
Gria2
Fmr1
correlation with renewal freezing

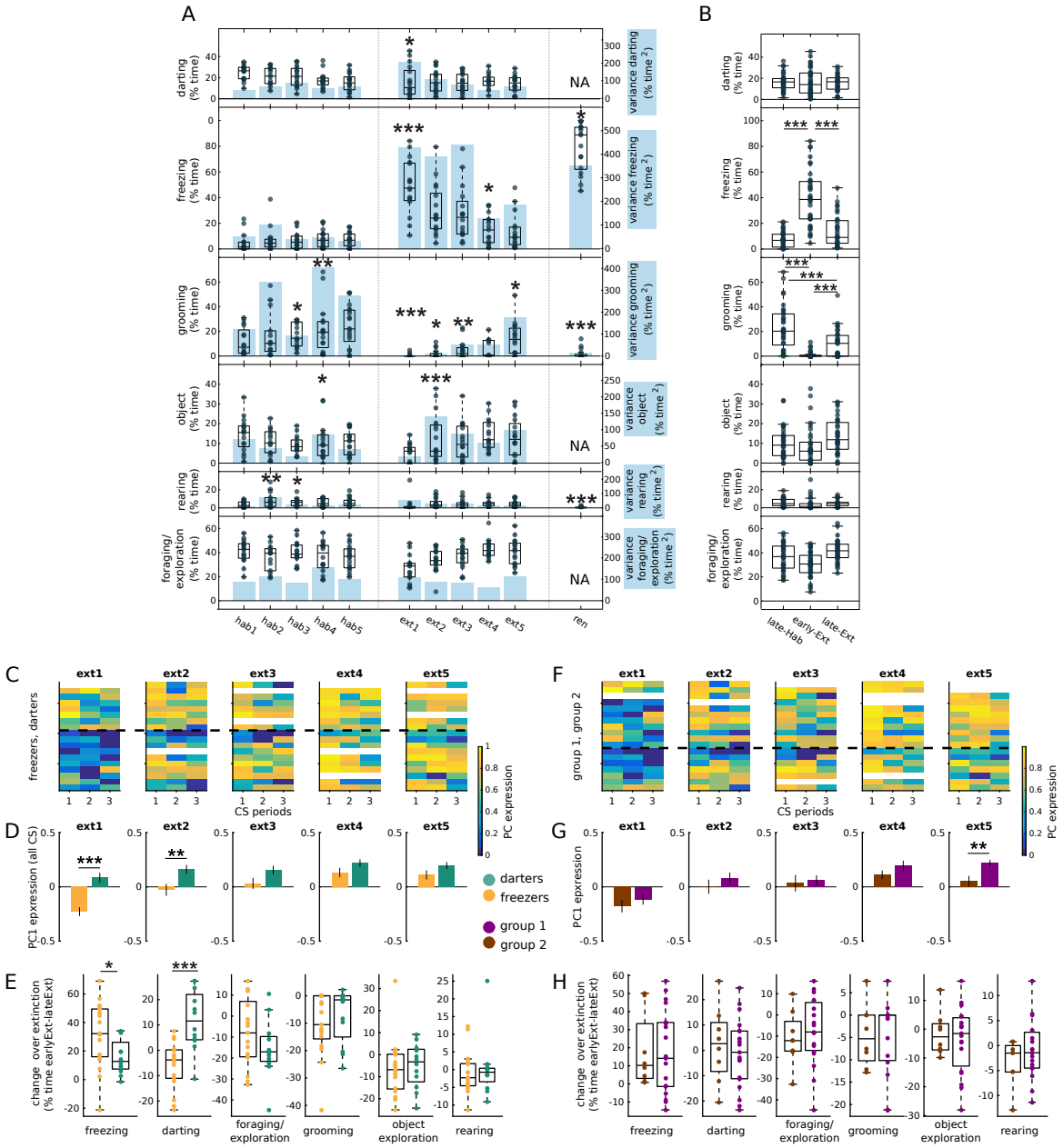

Figure S1. CS presentations elicited variable behavioral responses among animals (A-B). Segregating rats based on behavioral phenotype data from early extinction led to groups with significant differences of behavior evolution over extinction training (C-H). Relates to Figure 1.

(A) Time spent performing behaviors during CS periods and group variance. Dots represent individual rats' averages over the three CS periods. In box plots, the central bar indicates the median, the bottom and top edges indicate the 25th and 75th percentiles; whiskers extend to the most extreme data points, excluding outliers (see Methods). The blue shading bars depict variance (scales at right). Stars mark the sessions where the variance was different from the previous session (F-test for equal variances). Note that object exploration, darting, and other exploratory/foraging behavior could not be expressed (NA) in the small conditioning chamber.

(B) Comparison of behavioral expression during late habituation (late-Hab: hab4 and hab5), early extinction (early-Ext: ext1 and ext2), and late extinction (late-Ext: ext4 and ext5) sessions. Stars denote significant differences between these training stages (sign rank test). Only significant comparisons are shown.

(C-H) Segregating animals based on behavioral phenotype data from ext1 (C-E) but not from ext5 (F-H) led to groups with significant differences of behavior evolution over extinction training. (C) Evolution of PC1 values over the three CS periods in freezer and darter groups as clustered from ext1 data. Each row corresponds to one rat (white corresponds to unavailable data). Colors represent the average expression of PC1 for the respective CS presentations (numbered below). The horizontal dashed line separates the two groups (freezers and darters) determined from ext1 data. (D) Average values of PC1 expression over the sessions for the two groups. The expression of PC1 is significantly different between the two groups in ext1 (as expected) and also ext2 (unpaired t-test; $^{**}p<0.01$, $^{***}p<0.001$). (E) Changes in the behavior expression across extinction training sessions for the two groups as clustered with ext1 data. Colored dots represent the difference between early extinction (average of ext1 and ext2) and late extinction (average of ext4 and ext5). Note how the two groups manifest different evolution of the expression of freezing and darting over extinction training: darting extinguishes in darters and freezing change over extinction is greater for freezers. (F,G,H) Same as (C,D,E) but for the groups derived from k-means clustering on ext5 data. Note that the expression of PC1 differs between the two control groups only for the ext5 session used for clustering. Clustering with ext5 data did not lead to significant inter-group differences in behavioral expression changes over extinction.

Data is represented as mean ±SEM. Statistics are unpaired t-tests [$^{*}p<0.05$, $^{**}p<0.01$, $^{***}p<0.001$]

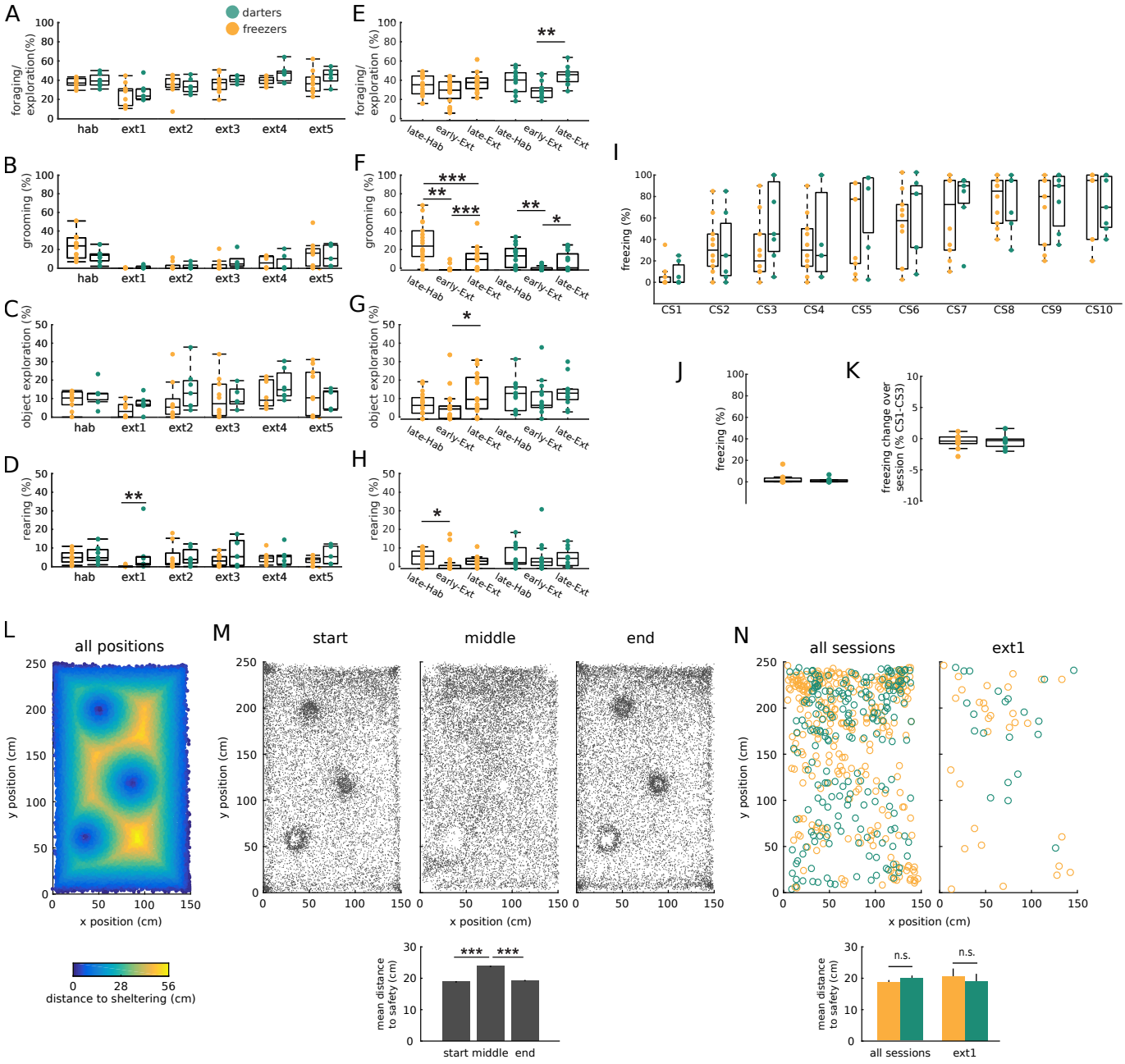

Figure S2. Comparison of expression of behaviors other than darting and freezing during CS periods across extinction training (A-D). Fear acquisition, generalization of contextual fear, and within-day learning rate do not explain interindividual variability during early extinction (I-K). Darting typically was from one 'sheltering' location to another (L-N). Relates to Figures 1 and 2.

(A-D) Equivalent of Figure 2A-B for other behaviors.

(E-H) Intra-group comparisons demonstrate significant differences in these behaviors expression over extinction learning (equivalent of Figure 2G-H for other behaviors).

(I) Percentage of time spent freezing during CS presentations in conditioning sessions (CS1-5 were presented on day 1 and CS6-10 on day 2).

(J) Percentage of time the animals spent freezing in baseline period prior to the first CS presentation in ext1.

(K) Differences between CS3 and CS1 for proportion of time spent freezing in ext1. No significant differences.

(L) Positions in the open field are colored according to their distance from the walls and the objects (all considered as 'sheltering' locations).

(M) Dots indicate all rats' positions at the beginning (top left), in the middle (top middle), and at the end (top right) of all darting trajectories for all sessions in one configuration of the open field (see Methods). (bottom) When in the middle of darting trajectories, rats were further away from sheltering locations ('safety') than at the beginning or end of trajectories.

(N) Positions of all rats (color coded by group) at CS onset for all sessions (left) and for ext1 (right). (bottom) No significant distance-to-safety difference between groups at CS onset.

Statistics are unpaired t-tests [n.s.:not significant; *p<0.05, **p<0.01, ***p<0.001]

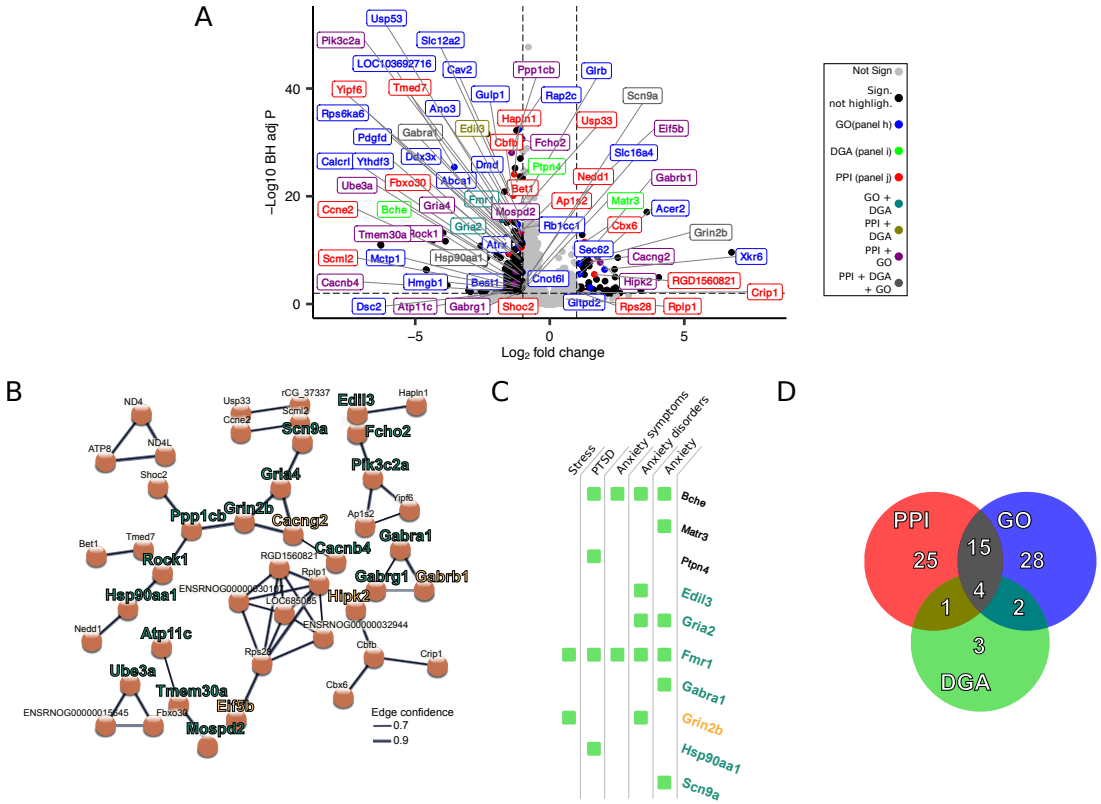

Figure S3. Differentially expressed genes (DEGs) in vmPFC between freezers and darters (A) and selection of DEGs more likely to play a role in the vulnerability to fear relapse (B-D). Relates to Figure 4.

(A) Volcano plot of the differential expression of the genes. Genes were considered to be significantly differentially expressed between groups if their adjusted P (Padj) was <0.01 (horizontal dotted line) and the absolute value of their Fold Change was >2 (vertical dotted lines). Non-DEGs are depicted by light gray dots. The colored lettering indicates DEGs retained by GO, PPI, and DGA analyses.

(B) PPI network of the DEGs obtained from STRING analysis of the DEGs list. Line thickness represents the confidence level supporting each protein–protein associations. Only connected nodes and interactions with confidence >0.7 are shown. The network has significantly more interactions than expected with a PPI enrichment p-value <0.02. Genes upregulated in freezers are in yellow while genes upregulated in darters are in green.

(C) DGA analysis using the DisGeNET database revealed DEGs previously associated with anxiety and stress-related disorders, indicated by the green squares. Gene label color-coding as in Figure 4.

(D) Venn diagram of the categories of the 78 DEGs selected by the GO Terms, PPI and DGA analyses.

See also Tables S1-2

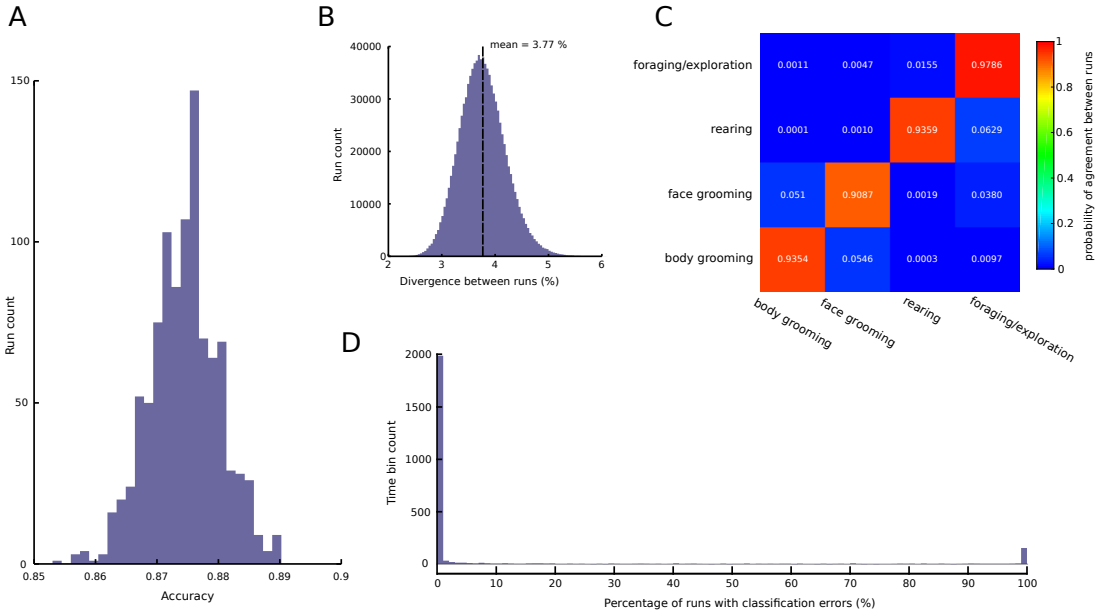

Figure S4. Performance and outcome consistency of supervised machine learning classification of behaviors from IMU and camera data over 1000 runs. Relates to STAR Methods.

(A) Classification accuracy distribution.

(B) Percent divergence between different runs of the machine learning classification. Results of the different runs were compared to each other, and for each comparison a divergence value was computed corresponding to the percentage of time bins with different classifications. On average, the different runs were different in 3.77% of the bins and the divergence was never greater than 6%.

(C) Conditional probability of classification. Colors represent the probability (also expressed numerically for each cell) that one run classified a time bin to a particular behavior, given the classification outcome for that bin from another run. For example, the top left cell indicates that the bins that were classified as ”foraging/exploration” on one run, had 0.001 (or 0.1%) probability of being classified as ”body grooming” on another run. Note the high values along the diagonal, indicating that time bins classified as a particular behavior on a given run are very likely to be classified as the same behavior on a different run, and therefore demonstrating consistency between runs.

(D) For each of the 2514 time bins of the test dataset, the proportion of runs when an error occurred was computed. Errors tend to concentrate in a few time bins and most time bins were never wrongly classified.

Gene Name	Base Mean	log2 Fold Change	Standard Error	Wald Statistic	Wald test p-value	BH adjusted p-value	dispersions dds	Monte Carlo p-value	selected by GO	selected by PPI	selected by DGA
0dk2	651.3505	-1.1010	0.1016	-10.8339	0.0000	0.0000	0.0156	0.0003	0	0	0
AABR07001896.1	29.4550	-1.0138	0.2150	-4.7147	0.0000	0.0001	0.0391	0.0003	0	0	0
AABR07001905.1	23.0908	-1.2473	0.3169	-3.9357	0.0001	0.0011	0.1166	0.0020	0	0	0
AABR07001910.1	30.9100	-1.7463	0.3645	-4.7906	0.0000	0.0000	0.1770	0.0003	0	0	0
AABR07001923.1	21.8214	-1.5873	0.2611	-6.0797	0.0000	0.0000	0.0528	0.0003	0	0	0
AABR07001926.3	59.7727	-1.7750	0.4785	-3.7093	0.0002	0.0023	0.3606	0.0090	0	0	0
AABR07005752.1	10.4440	-1.6862	0.4970	-3.3924	0.0007	0.0062	0.2811	0.0050	0	0	0
AABR07006627.1	19.7692	-2.3455	0.3552	-6.6023	0.0000	0.0000	0.1182	0.0003	0	0	0
AABR07007798.1	40.5005	-1.0195	0.3147	-3.2390	0.0012	0.0096	0.1382	0.0009	0	0	0
AABR07008066.2	57.0525	-1.5514	0.2009	-7.7214	0.0000	0.0000	0.0444	0.0003	0	0	0
AABR07012039.1	12.8124	6.7560	0.9692	6.9710	0.0000	0.0000	0.5589	<0.0002	0	0	0
AABR07012274.1	20.8024	1.7394	0.5387	3.2287	0.0012	0.0098	0.4212	0.0070	0	0	0
AABR07013802.1	11.5479	1.2185	0.3771	3.2313	0.0012	0.0098	0.1365	0.0047	0	0	0
AABR07014550.1	25.2002	1.4529	0.3190	4.5552	0.0000	0.0001	0.1210	<0.0002	0	0	0
AABR07017159.1	15.1696	1.3346	0.3820	3.4933	0.0005	0.0046	0.1652	0.0023	0	0	0
AABR07024457.1	23.8849	-1.2316	0.3200	-3.8491	0.0001	0.0015	0.1218	0.0020	0	0	0
AABR07026997.1	27.4838	1.7377	0.3578	4.8564	0.0000	0.0000	0.1648	0.0012	0	0	0
AABR07027212.1	72.2032	-1.4249	0.2869	-4.9665	0.0000	0.0000	0.1206	0.0009	0	0	0
AABR07029605.1	427.0017	-1.3173	0.1458	-9.0343	0.0000	0.0000	0.0328	0.0003	0	0	0
AABR07031480.1	58.4091	-1.0289	0.2331	-4.4148	0.0000	0.0002	0.0717	0.0009	0	0	0
AABR07033324.1	24.2898	-1.9771	0.2899	-6.8192	0.0000	0.0000	0.0764	0.0003	0	0	0
AABR07034657.1	13.3411	1.4451	0.3418	4.2279	0.0000	0.0004	0.1033	<0.0002	0	0	0
AABR07036007.1	55.3266	1.2773	0.2020	6.3241	0.0000	0.0000	0.0470	<0.0002	0	0	0
AABR07037058.2	35.1541	-1.8291	0.2762	-6.6233	0.0000	0.0000	0.0860	0.0003	0	0	0
AABR07043287.1	17.5367	-6.2728	0.8462	-7.4128	0.0000	0.0000	0.1979	0.0003	0	0	0
AABR07043288.1	17.6833	-6.2848	0.8415	-7.4689	0.0000	0.0000	0.1845	0.0003	0	0	0
AABR07043748.1	18.9974	3.6084	0.3909	9.2314	0.0000	0.0000	0.0757	<0.0002	0	0	0
AABR07049320.1	11.4980	-1.8629	0.3867	-4.8178	0.0000	0.0000	0.1199	0.0003	0	0	0
AABR07049329.1	11.4980	-1.8629	0.3867	-4.8178	0.0000	0.0000	0.1199	0.0003	0	0	0
AABR07055776.1	115.0931	-1.2481	0.2169	-5.7547	0.0000	0.0000	0.0685	0.0003	0	0	0
AABR07056515.1	21.4024	1.0295	0.2933	3.5105	0.0004	0.0043	0.0922	0.0023	0	0	0
AABR07058795.1	19.6716	-2.5619	0.3474	-7.3738	0.0000	0.0000	0.0973	0.0003	0	0	0
AABR07061383.1	12.3984	-4.3431	0.5635	-7.7075	0.0000	0.0000	0.0732	0.0003	0	0	0
AABR07073045.1	13.2370	-3.9622	0.4875	-8.1278	0.0000	0.0000	0.0597	0.0003	0	0	0
Abca1	251.6648	-1.1705	0.1564	-7.4842	0.0000	0.0000	0.0364	0.0003	1	0	0
AC099104.1	22.2189	1.2894	0.2430	5.3054	0.0000	0.0000	0.0458	<0.0002	0	0	0
AC103024.1	11.7251	-1.3281	0.3603	-3.6864	0.0002	0.0025	0.1110	0.0003	0	0	0
AC108578.1	27.7379	-1.2024	0.2427	-4.9550	0.0000	0.0000	0.0557	0.0003	0	0	0
AC111804.2	441.4262	-2.4535	0.2205	-11.1270	0.0000	0.0000	0.0773	0.0003	0	0	0
AC117869.1	15.6366	1.2425	0.3616	3.4364	0.0006	0.0054	0.1446	<0.0002	0	0	0
AC123471.1	14.4406	1.1714	0.2866	4.0876	0.0000	0.0006	0.0580	<0.0002	0	0	0
AC134224.3	5297.4881	4.0521	0.8028	5.0473	0.0000	0.0000	1.0830	0.0023	0	0	0
AC241873.1	78.3026	-1.5211	0.2214	-6.8705	0.0000	0.0000	0.0655	0.0009	0	0	0
Acer2	160.8773	1.1048	0.2070	5.3369	0.0000	0.0000	0.0650	<0.0002	1	0	0
Acss3	27.3591	-1.0489	0.2840	-3.6935	0.0002	0.0025	0.0934	0.0003	0	0	0
Actg2	34.1862	2.6087	0.7986	3.2665	0.0011	0.0089	1.0135	0.0006	0	0	0
Acvr2a	557.7121	-1.1506	0.3067	-3.7509	0.0002	0.0021	0.1561	0.0073	0	0	0
Ano3	1566.4407	-1.1019	0.1329	-8.2926	0.0000	0.0000	0.0289	0.0003	1	0	0
Ap1s2	336.3702	-1.0543	0.1285	-8.2036	0.0000	0.0000	0.0243	0.0003	0	1	0
Aqp4	3057.3347	-1.0673	0.1178	-9.0584	0.0000	0.0000	0.0230	0.0003	0	0	0
Atp11c	14.4107	-1.6474	0.4818	-3.4196	0.0006	0.0057	0.2939	0.0067	1	1	0
Atrx	1302.8827	-1.2799	0.1782	-7.1825	0.0000	0.0000	0.0525	0.0009	1	0	0
AY172581.1	53.0215	-1.1241	0.3327	-3.3790	0.0007	0.0064	0.1638	0.0003	0	0	0
AY172581.13	28.1682	-2.1213	0.4575	-4.6368	0.0000	0.0001	0.2919	0.0003	0	0	0
AY172581.14	266.6872	-1.0082	0.2975	-3.3888	0.0007	0.0062	0.1445	0.0009	0	0	0
AY172581.19	53.4758	-2.0748	0.4186	-4.9561	0.0000	0.0000	0.2636	0.0003	0	0	0
AY172581.2	21.9255	-1.1637	0.3258	-3.5719	0.0004	0.0036	0.1238	0.0003	0	0	0
AY172581.4	295.4383	-1.5307	0.3043	-5.0308	0.0000	0.0000	0.1511	0.0003	0	0	0
AY172581.6	451.8511	-1.3117	0.2782	-4.7146	0.0000	0.0001	0.1274	0.0003	0	0	0
B3galt2	673.5997	-1.0552	0.1728	-6.1060	0.0000	0.0000	0.0485	0.0009	0	0	0
Bche	71.4751	-1.1362	0.2136	-5.3192	0.0000	0.0000	0.0601	0.0003	0	0	1
Bclaf3	21.7554	-1.6852	0.3903	-4.3178	0.0000	0.0003	0.1917	0.0020	0	0	0
Best1	71.5264	-1.1122	0.2612	-4.2583	0.0000	0.0003	0.0982	0.0009	1	0	0
Bet1	315.7880	-1.0937	0.1151	-9.5013	0.0000	0.0000	0.0186	0.0003	0	1	0
Bmp5	13.1204	-1.3517	0.3675	-3.6782	0.0002	0.0026	0.1320	0.0015	0	0	0
C1galt1	268.2748	-1.7707	0.2004	-8.8342	0.0000	0.0000	0.0621	0.0003	0	0	0
Cacnb4	133.6601	-1.3797	0.4038	-3.4167	0.0006	0.0057	0.2647	0.0114	1	1	0
Cacng2	465.3060	1.4986	0.2374	6.3127	0.0000	0.0000	0.0920	<0.0002	1	1	0
Calcrl	131.6178	-1.4169	0.2378	-5.9576	0.0000	0.0000	0.0853	0.0003	1	0	0
Cav2	103.1524	-1.4947	0.1460	-10.2378	0.0000	0.0000	0.0231	0.0003	1	0	0
Cbfb	225.6998	-1.3625	0.1361	-10.0080	0.0000	0.0000	0.0256	0.0003	0	1	0
Cbx6	2159.2413	1.2937	0.1701	7.6061	0.0000	0.0000	0.0481	<0.0002	0	1	0
Ccdc122	17.3443	-1.1120	0.2525	-4.4043	0.0000	0.0002	0.0400	0.0003	0	0	0
Ccne2	45.4333	-1.4433	0.2939	-4.9115	0.0000	0.0000	0.1168	0.0009	0	1	0
Cd200r1	27.5930	-1.3429	0.3663	-3.6658	0.0002	0.0027	0.1802	0.0003	0	0	0
Cdh12	156.7053	-1.2953	0.2455	-5.2774	0.0000	0.0000	0.0934	0.0003	0	0	0
Cdh19	21.5415	-1.1903	0.2726	-4.3664	0.0000	0.0002	0.0696	0.0003	0	0	0
Cnot6l	101.6649	-1.0141	0.2014	-5.0361	0.0000	0.0000	0.0569	0.0009	1	0	0
Cobll1	97.2928	-1.2993	0.1473	-8.8189	0.0000	0.0000	0.0238	0.0003	0	0	0
Cpsf6	1245.7395	-1.2645	0.1355	-9.3348	0.0000	0.0000	0.0299	0.0003	0	0	0
Crip1	142.1265	1.1485	0.3463	3.3168	0.0009	0.0077	0.1935	0.0017	0	1	0
Cul4b	403.0531	-1.0826	0.2151	-5.0333	0.0000	0.0000	0.0749	0.0009	0	0	0
Cyyr1	179.2417	-1.1922	0.1835	-6.4989	0.0000	0.0000	0.0499	0.0003	0	0	0
Ddx3	776.0611	-1.8117	0.2541	-7.1312	0.0000	0.0000	0.1066	0.0009	0	0	0
Ddx3x	2019.2737	-1.1314	0.1564	-7.2363	0.0000	0.0000	0.0405	0.0003	1	0	0
Des	152.0469	1.6155	0.4287	3.7682	0.0002	0.0019	0.3004	0.0003	0	0	0
Dipk2a	1009.1935	-1.3034	0.1830	-7.1219	0.0000	0.0000	0.0551	0.0003	0	0	0
Dmd	890.5119	-1.1878	0.1382	-8.5915	0.0000	0.0000	0.0308	0.0003	1	0	0
Dsc2	14.7763	-1.6401	0.4881	-3.3602	0.0008	0.0068	0.3065	0.0009	1	0	0
Dsel	153.0079	-1.3715	0.2043	-6.7128	0.0000	0.0000	0.0619	0.0003	0	0	0
Edil3	1505.4647	-1.4016	0.1503	-9.3246	0.0000	0.0000	0.0371	0.0003	0	1	1
Eif5b	568.4272	1.2050	0.1201	10.0327	0.0000	0.0000	0.0222	<0.0002	1	1	0
Elavl2	694.2263	-1.1311	0.1247	-9.0735	0.0000	0.0000	0.0244	0.0003	0	0	0
Elavl3	546.0791	1.2628	0.2183	5.7837	0.0000	0.0000	0.0780	<0.0002	0	0	0
Ermn	143.9280	-1.0676	0.2536	-4.2103	0.0000	0.0004	0.1001	0.0009	0	0	0
Fam126b	374.8378	-1.2324	0.1547	-7.9664	0.0000	0.0000	0.0370	0.0003	0	0	0
Far1	608.0267	-1.1286	0.1994	-5.6603	0.0000	0.0000	0.0649	0.0009	0	0	0
Fbxo30	86.4030	-1.4944	0.2168	-6.8928	0.0000	0.0000	0.0638	0.0009	0	1	0
Fcho2	737.2980	-1.0246	0.0832	-12.3189	0.0000	0.0000	0.0101	0.0003	1	1	0
Fmr1	381.5531	-1.7693	0.1996	-8.8654	0.0000	0.0000	0.0631	0.0003	1	0	1
Fstl4	195.2104	1.2049	0.1997	6.0326	0.0000	0.0000	0.0611	<0.0002	0	0	0
G2e3	115.2957	-1.2427	0.2566	-4.8431	0.0000	0.0000	0.1001	0.0003	0	0	0
Gabra1	5078.9276	-1.1713	0.1545	-7.5802	0.0000	0.0000	0.0399	0.0003	1	1	1
Gabrb1	72.5263	1.3742	0.2016	6.8162	0.0000	0.0000	0.0514	<0.0002	1	1	0
Gabrg1	120.0816	-1.1629	0.3531	-3.2934	0.0010	0.0082	0.1997	0.0079	1	1	0
Gatm	815.5386	-1.0094	0.1456	-6.9336	0.0000	0.0000	0.0342	0.0003	0	0	0
Giot1	50.6077	-1.1714	0.2524	-4.6402	0.0000	0.0001	0.0837	0.0012	0	0	0

Gene Name	Base Mean	log2 Fold Change	Standard Error	Wald Statistic	Wald test p-value	BH adjusted p-value	dispersions dds	Monte Carlo p-value	selected by GO	selected by PPI	selected by DGA
Glrb	2588.1011	-1.0964	0.1151	-9.5248	0.0000	0.0000	0.0218	0.0003	1	0	0
Gltpd2	87.5283	1.4998	0.3743	4.0069	0.0001	0.0008	0.2210	0.0035	1	0	0
Gpm6a	21180.1139	-1.0956	0.0947	-11.5650	0.0000	0.0000	0.0150	0.0003	0	0	0
Gpr34	104.2433	-1.1080	0.1695	-6.5367	0.0000	0.0000	0.0371	0.0003	0	0	0
Gria2	7744.4910	-1.0943	0.1664	-6.5773	0.0000	0.0000	0.0464	0.0009	1	0	1
Gria4	1307.9248	-1.0949	0.1691	-6.4738	0.0000	0.0000	0.0472	0.0009	1	1	0
Grin2b	203.7624	1.7760	0.2671	6.6497	0.0000	0.0000	0.1131	<0.0002	1	1	1
Gtf2a1	78.4219	-1.4434	0.2312	-6.2441	0.0000	0.0000	0.0734	0.0009	0	0	0
Gulp1	57.8459	-1.9657	0.1611	-12.2005	0.0000	0.0000	0.0167	0.0003	1	0	0
Hapln1	566.1315	-1.3201	0.1208	-10.9299	0.0000	0.0000	0.0223	0.0003	0	1	0
Hipk2	68.0542	1.8731	0.2985	6.2751	0.0000	0.0000	0.1284	<0.0002	1	1	0
Hmgb1	19.0886	-1.3776	0.3595	-3.8324	0.0001	0.0016	0.1511	0.0003	1	0	0
Hsp90aa1	117.9233	-2.4189	0.3939	-6.1411	0.0000	0.0000	0.2445	0.0015	1	1	1
Jrkl	70.5917	-1.2115	0.2226	-5.4435	0.0000	0.0000	0.0663	0.0009	0	0	0
Kbtbd3	162.6595	-1.1651	0.1735	-6.7137	0.0000	0.0000	0.0433	0.0009	0	0	0
Kcnt2	488.7775	-1.3783	0.2416	-5.7054	0.0000	0.0000	0.0955	0.0009	0	0	0
Kitlg	336.8977	-1.0827	0.1914	-5.6583	0.0000	0.0000	0.0581	0.0009	0	0	0
Klhl4	120.3290	-1.4016	0.2347	-5.9706	0.0000	0.0000	0.0820	0.0015	0	0	0
Krt42	20.0015	1.1053	0.2707	4.0830	0.0000	0.0006	0.0662	<0.0002	0	0	0
Lmbrd2	38.4250	-1.6121	0.4615	-3.4935	0.0005	0.0046	0.3223	0.0096	0	0	0
LOC100360791	50.1358	-1.3667	0.2556	-5.3476	0.0000	0.0000	0.0845	0.0003	0	0	0
LOC102551340	48.1507	-1.3467	0.3721	-3.6188	0.0003	0.0031	0.2068	0.0047	0	0	0
LOC102552527	89.0346	-1.2328	0.2219	-5.5551	0.0000	0.0000	0.0692	0.0009	0	0	0
LOC102555377	174.2009	-1.4538	0.2681	-5.4221	0.0000	0.0000	0.1134	0.0009	0	0	0
LOC103692716	92.0557	-3.5474	0.3157	-11.2377	0.0000	0.0000	0.1290	0.0003	1	0	0
LOC500584	147.8921	-1.4291	0.1535	-9.3083	0.0000	0.0000	0.0309	0.0003	0	0	0
Lpar4	14.4156	-1.6649	0.3686	-4.5164	0.0000	0.0001	0.1328	0.0003	0	0	0
Lrif1	206.8141	-1.0368	0.1092	-9.4914	0.0000	0.0000	0.0145	0.0003	0	0	0
Lrrcc1	114.9924	-1.0112	0.1630	-6.2029	0.0000	0.0000	0.0348	0.0009	0	0	0
Lysmd3	37.5332	-1.6683	0.3490	-4.7803	0.0000	0.0000	0.1675	0.0009	0	0	0
Marcks	2186.6674	-1.0110	0.0938	-10.7820	0.0000	0.0000	0.0143	0.0003	0	0	0
Matr3	850.2008	-1.0100	0.2784	-3.6276	0.0003	0.0030	0.1290	0.0061	0	0	1
Mbnl2	2019.9007	-1.2902	0.1153	-11.1911	0.0000	0.0000	0.0217	0.0003	0	0	0
Mbtps2	262.7649	-1.0599	0.1716	-6.1751	0.0000	0.0000	0.0451	0.0009	0	0	0
Mctp1	193.7461	-1.1348	0.2821	-4.0227	0.0001	0.0008	0.1277	0.0026	1	0	0
Mdfic	20.6186	-1.5124	0.2968	-5.0959	0.0000	0.0000	0.0841	0.0003	0	0	0
Mei1	21.7524	1.0850	0.2930	3.7024	0.0002	0.0024	0.0920	0.0006	0	0	0
Mgat4c	85.8218	-1.2966	0.2162	-5.9960	0.0000	0.0000	0.0643	0.0015	0	0	0
MGC109340	561.6379	-1.6890	0.1658	-10.1882	0.0000	0.0000	0.0437	0.0003	0	0	0
Mier3	232.5463	-1.0558	0.2029	-5.2027	0.0000	0.0000	0.0643	0.0015	0	0	0
Mospd2	145.2221	-1.0817	0.1364	-7.9317	0.0000	0.0000	0.0233	0.0003	1	1	0
Mt-atp8	39993.4823	-1.5616	0.2509	-6.2248	0.0000	0.0000	0.1058	0.0003	0	0	0
Mt-nd4	1170.7632	-1.5401	0.1631	-9.4413	0.0000	0.0000	0.0436	0.0003	0	0	0
Mt-nd4l	5677.4989	-1.4115	0.1824	-7.7383	0.0000	0.0000	0.0557	0.0003	0	0	0
Necab1	2576.3288	-1.3221	0.2247	-5.8833	0.0000	0.0000	0.0844	0.0020	0	0	0
Nedd1	35.8092	-1.0320	0.2431	-4.2442	0.0000	0.0004	0.0672	0.0003	0	1	0
Npat	347.0868	-1.0867	0.2038	-5.3325	0.0000	0.0000	0.0665	0.0009	0	0	0
Olfm3	501.2336	-1.8869	0.2038	-9.2588	0.0000	0.0000	0.0668	0.0003	0	0	0
Pcdh20	427.7987	-1.1806	0.1500	-7.8699	0.0000	0.0000	0.0350	0.0003	0	0	0
Pcmtd2	1184.8999	-1.5062	0.2038	-7.3924	0.0000	0.0000	0.0687	0.0003	0	0	0
Pdgfd	43.4344	-1.5998	0.2022	-7.9127	0.0000	0.0000	0.0375	0.0003	1	0	0
Phf20l1	293.6658	-1.1404	0.2373	-4.8065	0.0000	0.0000	0.0906	0.0020	0	0	0
Pik3c2a	312.9221	-1.1102	0.1449	-7.6630	0.0000	0.0000	0.0315	0.0003	1	1	0
Plagl1	59.3202	-1.6129	0.3085	-5.2277	0.0000	0.0000	0.1369	0.0015	0	0	0
Ppial4d	21.0191	-1.5836	0.3177	-4.9848	0.0000	0.0000	0.1049	0.0003	0	0	0
Ppp1cb	3925.3016	-1.4177	0.1203	-11.7843	0.0000	0.0000	0.0240	0.0003	1	1	0
Prrg1	61.5919	-2.3273	0.1860	-12.5097	0.0000	0.0000	0.0283	0.0003	0	0	0
Ptchd1	191.6880	-1.0834	0.1658	-6.5338	0.0000	0.0000	0.0402	0.0009	0	0	0
Ptpn4	824.7156	-1.2414	0.1170	-10.6125	0.0000	0.0000	0.0215	0.0003	0	0	1
Pwwp3b	28.6260	-1.2260	0.2536	-4.8343	0.0000	0.0000	0.0663	0.0003	0	0	0
Rap2c	637.3930	-1.1524	0.0906	-12.7131	0.0000	0.0000	0.0120	0.0003	1	0	0
Rb1cc1	1078.4385	-1.0192	0.1216	-8.3787	0.0000	0.0000	0.0238	0.0003	1	0	0
Rbm39	13.6561	-3.8763	0.5063	-7.6560	0.0000	0.0000	0.1180	0.0003	0	0	0
RF00152	19.8914	-1.7320	0.3900	-4.4409	0.0000	0.0002	0.1834	0.0003	0	0	0
RF00592	42.3630	-1.3549	0.2655	-5.1036	0.0000	0.0000	0.0889	0.0003	0	0	0
Rfx7	455.9730	-1.0353	0.1757	-5.8926	0.0000	0.0000	0.0494	0.0009	0	0	0
RGD1560821	24.1176	1.6552	0.3112	5.3197	0.0000	0.0000	0.1071	<0.0002	0	1	0
RGD1565622	29.6663	-1.4992	0.3179	-4.7157	0.0000	0.0001	0.1258	0.0015	0	0	0
RGD1566265	112.3414	-1.0961	0.2730	-4.0153	0.0001	0.0008	0.1149	0.0023	0	0	0
Ro60	17.2220	-1.7885	0.4597	-3.8904	0.0001	0.0013	0.2705	0.0009	0	0	0
Rock1	2038.8320	-1.0951	0.2408	-4.5477	0.0000	0.0001	0.0969	0.0020	1	1	0
Rps28	989.4499	1.0059	0.2882	3.4899	0.0005	0.0046	0.1386	0.0076	0	1	0
Rps6ka6	74.6348	-1.6464	0.2131	-7.7256	0.0000	0.0000	0.0578	0.0003	1	0	0
Rsbn1	362.7275	-1.3267	0.1611	-8.2328	0.0000	0.0000	0.0402	0.0003	0	0	0
Scml2	13.1429	-1.6128	0.3935	-4.0983	0.0000	0.0006	0.1569	0.0009	0	1	0
Scn9a	82.7024	-1.0356	0.2582	-4.0110	0.0001	0.0008	0.0982	0.0026	1	1	1
Sec62	1918.8733	1.0931	0.1764	6.1982	0.0000	0.0000	0.0517	<0.0002	1	0	0
Sema3c	824.9659	-1.0571	0.1575	-6.7116	0.0000	0.0000	0.0403	0.0003	0	0	0
Senp7	202.6915	-1.0579	0.1683	-6.2872	0.0000	0.0000	0.0419	0.0009	0	0	0
Shoc2	349.2864	-1.0879	0.3008	-3.6163	0.0003	0.0031	0.1488	0.0055	0	1	0
Slc12a2	672.6355	-1.1315	0.1247	-9.0724	0.0000	0.0000	0.0244	0.0003	1	0	0
Slc16a4	30.8257	-1.0676	0.2897	-3.6848	0.0002	0.0025	0.1035	0.0003	1	0	0
Slc5a7	34.5165	-1.1262	0.2512	-4.4838	0.0000	0.0001	0.0722	0.0009	0	0	0
Spock3	585.6549	-1.3294	0.1992	-6.6745	0.0000	0.0000	0.0646	0.0003	0	0	0
St18	30.8126	-1.1869	0.3205	-3.7029	0.0002	0.0024	0.1341	0.0003	0	0	0
Stk26	21.4131	-1.1892	0.2842	-4.1836	0.0000	0.0005	0.0806	0.0009	0	0	0
Strn3	791.2540	-1.1159	0.2000	-5.5808	0.0000	0.0000	0.0657	0.0009	0	0	0
Tbc1d15	379.5415	-1.0950	0.1861	-5.8848	0.0000	0.0000	0.0551	0.0009	0	0	0
Tbc1d8b	73.8496	-1.2635	0.2061	-6.1311	0.0000	0.0000	0.0549	0.0009	0	0	0
Tc2n	21.9810	-1.4217	0.3293	-4.3173	0.0000	0.0003	0.1244	0.0026	0	0	0
Tceal5	194.6831	1.2042	0.1498	8.0393	0.0000	0.0000	0.0317	<0.0002	0	0	0
Tmed7	729.9032	-1.5676	0.1794	-8.7400	0.0000	0.0000	0.0522	0.0003	0	1	0
Tmem158	60.3717	1.0837	0.3014	3.5959	0.0003	0.0033	0.1339	0.0023	0	0	0
Tmem196	768.8871	-1.3098	0.1504	-8.7103	0.0000	0.0000	0.0364	0.0003	0	0	0
Tmem30a	1124.4566	-1.3116	0.2969	-4.4172	0.0000	0.0002	0.1471	0.0020	1	1	0
Tmem47	1503.4855	-1.2332	0.0975	-12.6497	0.0000	0.0000	0.0152	0.0003	0	0	0
Tmsb10	34.7354	2.4089	0.4193	5.7456	0.0000	0.0000	0.2428	<0.0002	0	0	0
Togaram1	844.6871	-1.0651	0.1921	-5.5439	0.0000	0.0000	0.0607	0.0009	0	0	0
Trim59	75.5956	-1.2720	0.2171	-5.8597	0.0000	0.0000	0.0630	0.0003	0	0	0
Tspan12	448.1605	-1.0696	0.1018	-10.5071	0.0000	0.0000	0.0148	0.0003	0	0	0
Tug1	85.8764	-1.0124	0.2168	-4.6701	0.0000	0.0001	0.0657	0.0003	0	0	0
Ube3a	234.6795	-1.2616	0.2262	-5.5769	0.0000	0.0000	0.0808	0.0009	1	1	0
Usp33	1889.7712	-1.0020	0.1069	-9.3708	0.0000	0.0000	0.0186	0.0003	0	1	0
Usp51	19.3002	2.5300	0.3826	6.6126	0.0000	0.0000	0.1466	<0.0002	0	0	0
Usp53	275.0914	-1.0347	0.1363	-7.5940	0.0000	0.0000	0.0270	0.0003	1	0	0
Vgll4	151.0303	1.4054	0.2156	6.5169	0.0000	0.0000	0.0700	<0.0002	0	0	0
Wdr44	197.5540	-1.0392	0.2512	-4.1367	0.0000	0.0005	0.1003	0.0032	0	0	0

Gene Name	Base Mean	log2 Fold Change	Standard Error	Wald Statistic	Wald test p-value	BH adjusted p-value	dispersions dds	Monte Carlo p-value	selected by GO	selected by PPI	selected by DGA
Xkr6	12.8746	2.0377	0.3558	5.7278	0.0000	0.0000	0.0930	$<$0.0002	1	0	0
Yipf4	273.8324	-1.0229	0.1364	-7.4971	0.0000	0.0000	0.0271	0.0003	0	0	0
Yipf6	592.3460	-1.0540	0.1448	-7.2785	0.0000	0.0000	0.0333	0.0003	0	1	0
Ythdf3	525.9740	-1.0140	0.1841	-5.5077	0.0000	0.0000	0.0548	0.0009	1	0	0
Zbed5	294.8049	1.4666	0.2442	6.0061	0.0000	0.0000	0.0960	$<$0.0002	0	0	0
Zbtb6	86.0060	-1.5863	0.3937	-4.0286	0.0001	0.0008	0.2449	0.0055	0	0	0
Zc2hc1a	808.6106	-1.0156	0.1132	-8.9694	0.0000	0.0000	0.0201	0.0003	0	0	0
Zdhhc20	89.8214	-1.2236	0.3493	-3.5025	0.0005	0.0044	0.1917	0.0073	0	0	0
Zfp367	279.7605	-1.0911	0.1397	-7.8110	0.0000	0.0000	0.0286	0.0003	0	0	0
Zfp40	261.0645	-1.3110	0.2080	-6.3027	0.0000	0.0000	0.0680	0.0003	0	0	0
Zfp458	28.4926	-1.5113	0.2757	-5.4812	0.0000	0.0000	0.0818	0.0003	0	0	0
Zfp51	81.4555	-1.3376	0.2210	-6.0523	0.0000	0.0000	0.0668	0.0009	0	0	0
Zfp518a	66.1255	-1.0427	0.2519	-4.1390	0.0000	0.0005	0.0893	0.0003	0	0	0
Zfp52	30.0754	-1.6594	0.2876	-5.7706	0.0000	0.0000	0.0928	0.0003	0	0	0
Zfp536	101.3186	1.3775	0.2046	6.7339	0.0000	0.0000	0.0582	$<$0.0002	0	0	0
Zfp600	89.7770	-1.5874	0.1828	-8.6833	0.0000	0.0000	0.0411	0.0003	0	0	0
Zfp711	136.3343	-1.4466	0.2423	-5.9693	0.0000	0.0000	0.0892	0.0009	0	0	0
Zfp800	76.9866	-1.1677	0.1997	-5.8476	0.0000	0.0000	0.0516	0.0009	0	0	0
Zfp950	27.2073	-1.1520	0.3247	-3.5474	0.0004	0.0039	0.1340	0.0015	0	0	0
Zfpm2	160.8647	-1.0532	0.1913	-5.5051	0.0000	0.0000	0.0544	0.0003	0	0	0
Zfr	3318.3402	-1.0838	0.1458	-7.4328	0.0000	0.0000	0.0354	0.0003	0	0	0
Zfx	199.2253	-1.0834	0.1675	-6.4687	0.0000	0.0000	0.0413	0.0003	0	0	0
Zkscan8	207.6151	-1.1024	0.1914	-5.7604	0.0000	0.0000	0.0559	0.0009	0	0	0
Zmym5	275.0641	-1.0234	0.2576	-3.9729	0.0001	0.0010	0.1074	0.0035	0	0	0

Table S1. Summary of all Differentially Expressed Genes (DEGs) and corresponding statistics. Relates to Figure 4 and Figure S3
Genes are ordered alphabetically and corresponding rows are colored in green or yellow for genes expressed more in darters or freezers, respectively. In the last three columns the number 1 indicates that the corresponding gene was selected by GO, PPI, or DGA analyses.

A

GO Term	Description	LogP	Log(q-value)	InTerm InList	Genes
0007214	**GABA signaling pathway**	-5.1983	-0.994	5/28	Gabrb1,Gabra1,Cacnb4,Slc12a2,Gabrg1
1902476	chloride transmembrane transport	-4.3535	-0.451	7/98	Gabrb1,Glrb,Gabra1,Slc12a2,Gabrg1,Best1,Ano3
0006821	chloride transport	-4.0088	-0.282	7/111	Gabrb1,Glrb,Gabra1,Slc12a2,Gabrg1,Best1,Ano3
0098661	inorganic anion transmembrane transport	-3.7522	-0.205	7/122	Gabrb1,Glrb,Gabra1,Slc12a2,Gabrg1,Best1,Ano3
0015698	inorganic anion transport	-2.8885	0.000	7/170	Gabrb1,Glrb,Gabra1,Slc12a2,Gabrg1,Best1,Ano3
0009582	detection of abiotic stimulus	-2.7107	0.000	6/135	Grin2b,Fmr1,Cacnb4,Slc12a2,Best1,Ano3
0009581	detection of external stimulus	-2.6945	0.000	6/136	Grin2b,Fmr1,Cacnb4,Slc12a2,Best1,Ano3
0006820	anion transport	-2.4177	0.000	14/645	Grin2b,Gabrb1,Glrb,Gabra1,Cacnb4,Slc12a2,Gabrg1, Best1,Slc16a4,Tmem30a,Ano3,Abca1,Atp11c,Gltpd2
0050982	detection of mechanical stimulus	-2.4053	0.000	4/67	Grin2b,Fmr1,Slc12a2,Ano3
0042391	**regulation of membrane potential**	-3.6790	-0.205	14/476	Grin2b,Dmd,Fmr1,Gabrb1,Glrb,Gria2,Gria4, Gabra1,Cacnb4,Scn9a,Cacng2,Gabrg1,Dsc2,Usp53
0001508	action potential	-3.3129	0.000	7/144	Grin2b,Dmd,Fmr1,Cacnb4,Scn9a,Dsc2,Usp53
1901385	regulation of voltage-gated calcium channel activity	-2.1489	0.000	3/41	Dmd,Fmr1,Cacnb4
0097035	**regulation of membrane lipid distribution**	-3.6307	-0.205	5/58	Tmem30a,Xkr6,Ano3,Abca1,Atp11c
0045332	phospholipid translocation	-2.6679	0.000	3/27	Tmem30a,Abca1,Atp11c
0034204	lipid translocation	-2.5346	0.000	3/30	Tmem30a,Abca1,Atp11c
0015914	phospholipid transport	-2.3151	0.000	4/71	Tmem30a,Abca1,Atp11c,Gltpd2
0005980	**glycogen catabolic process**	-3.0557	0.000	3/20	Hmgb1,Ppp1cb,Rb1cc1
0009251	glucan catabolic process	-3.0557	0.000	3/20	Hmgb1,Ppp1cb,Rb1cc1
0044247	cellular polysaccharide catabolic process	-2.9918	0.000	3/21	Hmgb1,Ppp1cb,Rb1cc1
0000272	polysaccharide catabolic process	-2.9312	0.000	3/22	Hmgb1,Ppp1cb,Rb1cc1
0044275	cellular carbohydrate catabolic process	-2.2096	0.000	3/39	Hmgb1,Ppp1cb,Rb1cc1
0060078	**regulation of postsynaptic membrane potential**	-3.0257	0.000	7/161	Grin2b,Gabrb1,Glrb,Gria2,Gria4,Gabra1,Gabrg1
0035235	ionotropic glutamate receptor signaling pathway	-2.5773	0.000	3/29	Grin2b,Gria2,Gria4
0060992	response to fungicide	-2.4538	0.000	3/32	Grin2b,Gria2,Gria4
0007215	glutamate receptor signaling pathway	-2.4115	0.000	5/108	Grin2b,Fmr1,Gria2,Gria4,Cacng2
0031954	**positive regulation of protein autophosphorylation**	-2.6679	0.000	3/27	Pdgfd,Rap2c,Ddx3x
0071677	**positive regulation of mononuclear cell migration**	-2.5773	0.000	3/29	Hmgb1,Pdgfd,Mospd2
0061157	**mRNA destabilization**	-2.4538	0.000	3/32	Rock1,Cnot6l,Ythdf3
0050779	RNA destabilization	-2.3425	0.000	3/35	Rock1,Cnot6l,Ythdf3
0006446	**regulation of translational initiation**	-2.4288	0.000	4/66	Fmr1,Eif5b,Ddx3x,Ythdf3
0044788	**modulation by host of viral process**	-2.4154	0.000	3/33	Fmr1,Ddx3x,Cav2
0006413	translational initiation	-2.2336	0.000	5/119	Fmr1,Eif5b,Ddx3x,Ythdf3,Eif5b-ps1
0030330	**DNA damage response, signal transduction by p53 class mediator**	-2.3821	0.000	4/68	Atrx,Acer2,Rps6ka6,Hipk2
0071806	**protein transmembrane transport**	-2.3821	0.000	4/68	Sec62,Hsp90aa1,Abca1,LOC103692716
0006897	**endocytosis**	-2.2684	0.000	14/671	Fmr1,Calcrl,Hmgb1,Gria2,Rock1,Cacng2,Xkr6, Fcho2,Mctp1,Abca1,Gulp1,Ube3a,Pik3c2a,Cav2

GO Term	Description	LogP	Log(q-value)	InTerm InList	Genes
0010324	membrane invagination	-2.0411	0.000	4/85	Xkr6,Fcho2,Abca1,Gulp1
0042220	**response to cocaine**	-2.1905	0.000	4/77	Grin2b,Fmr1,Hsp90aa1,Ube3a
0060359	response to ammonium ion	-2.0242	0.000	6/187	Grin2b,Fmr1,Gabrb1,Gabra1,Hsp90aa1,Ube3a
0007628	**adult walking behavior**	-2.0105	0.000	3/46	Glrb,Cacnb4,Hipk2

B

Node 1	Node 2	Neighborhood on chromosome	Homology	Coexpression	Experimentally determined interaction	Database annotated	Automated textmining	Combined score
ATP8	ND4L	0	0	0.718	0	0	0.878	0.964
ATP8	ND4	0	0	0.248	0	0	0.860	0.890
Ap1s2	Yipf6	0	0	0.083	0	0.900	0.049	0.905
Ap1s2	Pik3c2a	0	0	0.045	0	0.900	0.043	0.900
Atp11c	Tmem30a	0	0	0.087	0.222	0	0.664	0.741
Bet1	Tmed7	0	0	0.110	0	0.900	0.078	0.910
Cacnb4	Cacng2	0	0	0.098	0	0.900	0.273	0.928
Cacng2	Grin2b	0	0	0.167	0.127	0.900	0.584	0.965
Cacng2	Gria4	0	0	0.126	0.403	0.900	0.838	0.990
Cbfb	Crip1	0	0	0.063	0.806	0	0	0.810
Cbfb	Hipk2	0	0	0	0	0.900	0.058	0.901
Cbfb	Cbx6	0	0	0.062	0	0.900	0	0.902
Ccne2	Scml2	0	0	0.064	0.780	0	0	0.785
ENSRNOG00000015645	Fbxo30	0	0	0.111	0	0.900	0	0.907
ENSRNOG00000015645	Ube3a	0	0	0.063	0.051	0.900	0.065	0.905
ENSRNOG00000030107	Rplp1	0	0	0.540	0.615	0	0.151	0.836
ENSRNOG00000030107	LOC685085	0	0	0.468	0.489	0	0.075	0.726
ENSRNOG00000030107	RGD1560821	0	0	0.532	0.605	0	0.126	0.824
ENSRNOG00000030107	Rps28	0	0	0.526	0.606	0	0.191	0.835
ENSRNOG00000032944	Rplp1	0	0	0.540	0.615	0	0.151	0.836
ENSRNOG00000032944	Rps28	0	0	0.526	0.606	0	0.191	0.835
ENSRNOG00000032944	LOC685085	0	0	0.468	0.489	0	0.075	0.726
ENSRNOG00000032944	RGD1560821	0	0	0.532	0.605	0	0.126	0.824
Edil3	Hapln1	0	0	0.108	0	0	0.834	0.846
Eif5b	Rps28	0.092	0	0.081	0.917	0	0.126	0.931
Fbxo30	Ube3a	0	0	0.064	0	0.900	0	0.902
Fcho2	Pik3c2a	0	0	0.087	0	0.900	0.059	0.906
Gabra1	Gabrb1	0	0.813	0.223	0.649	0.900	0.761	0.974
Gabra1	Gabrg1	0	0.911	0.271	0.215	0.540	0.661	0.730
Gabrb1	Gabrg1	0	0.844	0.226	0.396	0.540	0.904	0.799
Gria4	Scn9a	0	0	0.140	0.066	0.900	0.190	0.926
Gria4	Grin2b	0	0.700	0.221	0.140	0.900	0.696	0.942
Grin2b	Ppp1cb	0	0	0	0.083	0.800	0.103	0.821
Hsp90aa1	Nedd1	0	0	0	0	0.900	0	0.900
Hsp90aa1	Rock1	0	0	0.080	0.176	0.900	0.118	0.924
LOC685085	Rplp1	0	0	0.543	0.615	0	0.130	0.833
LOC685085	Rps28	0	0	0.526	0.605	0	0.213	0.839
LOC685085	RGD1560821	0	0	0.534	0.605	0	0.106	0.821
Mospd2	Tmem30a	0	0	0.080	0.144	0.900	0	0.914
ND4	ND4L	0	0	0.799	0.871	0.360	0.955	0.999
Pik3c2a	Yipf6	0	0	0.064	0	0.900	0	0.902
Ppp1cb	Rock1	0.042	0	0.086	0.163	0.800	0.112	0.846
Ppp1cb	Shoc2	0	0	0.064	0.238	0.720	0.422	0.869
RGD1560821	Rplp1	0	0	0.571	0.742	0	0.101	0.891
RGD1560821	Rps28	0.088	0	0.558	0.645	0	0.128	0.858
Rplp1	Rps28	0	0	0.855	0.742	0	0.327	0.972
Usp33	rCG_37337	0	0	0.799	0	0	0.067	0.805

C

Disease	Disease id	Gene	Gene Name	Disease Specificity Index	Disease Pleiotropy Index	pLI	GDA Score	# PMIDs	First PMID	Last PMID
Anxiety	C0003467	BCHE	butyrylcholinesterase	0.447	0.923	1.06E-13	0.05	5	2017	2019
Anxiety	C0003467	FMR1	FMRP translational regulator 1	0.473	0.769	0.64718	0.2	11	2002	2019
Anxiety	C0003467	GABRA1	GABA A receptor subunit alpha1	0.563	0.577	0.91489	0.1	0	NA	NA
Anxiety	C0003467	GRIA2	glutamate ionotropic receptor AMPA subunit 2	0.573	0.692	0.99916	0.01	1	2010	2010

Disease	Disease id	Gene	Gene Name	Disease Specificity Index	Disease Pleiotropy Index	pLI	GDA Score	# PMIDs	First PMID	Last PMID
Anxiety	C0003467	MATR3	matrin 3	0.631	0.538	1	0.1	0	NA	NA
Anxiety	C0003467	SCN9A	sodium voltage-gated channel alpha subunit 9	0.543	0.615	4.75E-19	0.1	0	NA	NA
Anxiety Disorders	C0003469	BCHE	butyrylcholinesterase	0.447	0.923	1.06E-13	0.05	5	2017	2019
Anxiety Disorders	C0003469	EDIL3	EGF like repeats and discoidin domains 3	0.564	0.769	0.00014584	0.1	1	2019	2019
Anxiety Disorders	C0003469	FMR1	FMRP translational regulator 1	0.473	0.769	0.64718	0.4	16	2002	2019
Anxiety Disorders	C0003469	GRIA2	glutamate ionotropic receptor AMPA subunit 2	0.573	0.692	0.99916	0.01	1	2010	2010
Anxiety Disorders	C0003469	GRIN2B	glutamate ionotropic receptor NMDA subunit 2B	0.51	0.692	1	0.01	1	2019	2019
Anxiety symptoms	C0860603	BCHE	butyrylcholinesterase	0.447	0.923	1.06E-13	0.01	1	2019	2019
Anxiety symptoms	C0860603	FMR1	FMRP translational regulator 1	0.473	0.769	0.64718	0.01	1	2012	2012
Post-Traumatic Stress Disorder	C0038436	BCHE	butyrylcholinesterase	0.447	0.923	1.06E-13	0.01	1	2017	2017
Post-Traumatic Stress Disorder	C0038436	FMR1	FMRP translational regulator 1	0.473	0.769	0.64718	0.01	1	2009	2009
Post-Traumatic Stress Disorder	C0038436	HSP90AA1	heat shock protein 90 alpha family class A member 1	0.411	0.923	0.86025	0.02	2	2011	2018
Post-Traumatic Stress Disorder	C0038436	PTPN4	protein tyrosine phosphatase non-receptor type 4	0.633	0.538	0.99663	0.01	1	2018	2018
Stress, Psychological	C0038443	FMR1	FMRP translational regulator 1	0.473	0.769	0.64718	0.01	1	2012	2012
Stress, Psychological	C0038443	GRIN2B	glutamate ionotropic receptor NMDA subunit 2B	0.51	0.692	1	0.01	1	2019	2019

Table S2. Summary of genes highlighted by GO, STRING, and PPI analyses. Relates to Figure 4 and Figure S3.

(A) Summary of GO analysis results. Significantly enriched Biological Processes GO terms are represented. P-values were calculated based on the accumulative hypergeometric distribution, and q-values were calculated using the Benjamini-Hochberg procedure to account for multiple testing using Metascape. The portion of genes associated with each GO term that was identified within the DEGs are reported and their symbols are detailed. Horizontal lines separate groups of GO terms whose summary term is indicated in bold.

(B) STRING analysis summary and statistics. Each protein-protein interaction that is part of the PPI network of the DEGs obtained from STRING analysis of the DEGs list is described. Only connected nodes and interactions with confidence >0.7 are described. The strength of data supporting each association is reported as well as the type of connection: Neighborhood on chromosome, Homology, Co-expression, Experimentally determined interaction, Analysis of database information, Automated text mining of co-occurrence of gene/protein names.

(C) Summary of DGA analysis results and statistics. List of DEGs that have been previously associated with anxiety and stress-related disorders according to DGA analysis (DisGeNET database). The Disease Specificity Index (DSI) reflects whether genes are associated to several or fewer diseases and the Disease Pleiotropy Index (DPI) reveals whether these diseases are similar or not. The probability of being loss-of-function (LoF) intolerant (pLI) measures how much the naturally occurring LoF variation has been depleted from a gene by natural selection. LoF intolerant genes will have a high pLI value (>0.9). The GDA score indicates the level of evidence of the association based on the number and type of sources.